# POST BUCKLING ANALYSIS OF CENTRELINE STIFFENED FLAT RECTANGULAR PLATES

A Thesis Submitted to

Indian Institute of Technology Hyderabad

In Partial Fulfillment of the Requirements for

The Degree of Master of Technology

**by**

## JOFIN GEORGE

भारतीय प्रौद्योगिकी संस्थान हैदराबाद
**Indian Institute of Technology Hyderabad**

to the

Department of Civil Engineering

Indian Institute of Technology Hyderabad

June, 2015

Supervisor : Dr. Mahendrakumar Madhavan

i

# Declaration

I declare that this written submission represents my ideas in my own words, and where others ideas or words have been included, I have adequately cited and referenced the original sources. I also declare that I have adhered to all principles of academic honesty and integrity and have not misrepresented or fabricated or falsified any idea/data/fact/source in my submission. I understand that any violation of the above will be a cause for disciplinary action by the Institute and can also evoke penal action from the sources that have thus not been properly cited, or from whom proper permission has not been taken when needed
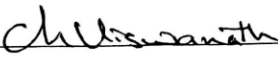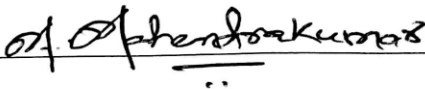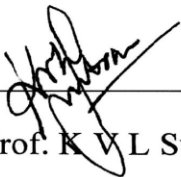
Jofin George

CE13M1007

# Approval Sheet

This thesis entitled **Post buckling analysis of centerline stiffened flat rectangular plates** by Jofin George is approved for the degree of Master of Technology from IIT Hyderabad.
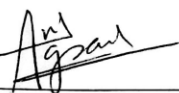
Dr. Viswanath Chinthapenta

Examiner

Dr. Mahendrakumar Madhavan

Advisor

Prof. K V L Subramaniam

Examiner

Dr. Anil Agarwal

Examiner

Dr. S Suriya Prakash

Examiner

# ABSTRACT

Centerline stiffened plates with eccentric compression is common in civil engineering structures. A detailed study is required in the post buckling behavior and stress distribution of centerline stiffened flat plate. For the effective utilization of plate material the post buckling behavior of the eccentrically compressed plate need to be studied in detail. As an initial phase a detailed study on post buckling behavior of flat plates simply supported on all four edges is completed which was done by A.C Walker (1967). A rectangular plate with centerline rotational restraint is considered in stage 2 of the work. An approximate solution for Von Karman equation for post buckling region of an initially flat rectangular plate subjected to non-uniform in plane axial compression is found out using Galerkin's method. The centerline of the plate is rotationally restraint. The loaded edges are simply supported and the unloaded edges are free. A series approximation is made for the stress function as well as the deflection series. The relation between edge compressive stress, applied load and the deflection profile is illustrated. Expressions for effective width of the centerline stiffened plate is proposed. The effect of varying number of terms in the stress function as well as the deflection function series is also studied for the above illustration. Till date very little information is available on post buckling response of a centerline stiffened initially flat rectangular plate. This work is an effort to fill this gap.

# Acknowledgements

# TABLE OF CONTENT

# TABLE OF CONTENT (Continued)

# LIST OF FIGURES

## LIST OF SYMBOLS

| | |
|---|---|
| b | plate width |
| $b_{ij}$ | stress function coefficient |
| D | flexural stiffness of the plate |
| E | Young's modulus of the plate |
| F | Airy's stress function |
| F' | Non dimensional form of Airy's stress function |
| k | buckling coefficient |
| l | plate length |
| m | number of half sine waves in $\xi$ direction |
| No | normal force per unit length along loaded edge |
| No' | Non dimensional form of No |
| $q_{ij}$ | deflection function coefficient |
| t | thickness of the plate |
| w | middle surface deflection of the plate along z direction |
| x,y,z | Cartesian coordinates |
| $\alpha$ | load eccentricity parameter |
| $\xi, \eta$ | non dimensional Cartesian coordinates |
| $\omega$ | non dimensional form of displacement |
| $\varphi$ | aspect ratio of the plate given by $\varphi = l/b$ |
| $\omega$ | non dimensional displacement given by $\omega = w/t$ |

| r | degree of rotational stiffness per unit distance in x direction |
| $\Gamma$ | non dimensional rotational restraint of the plate given by |
| | $\Gamma = rb/D$ |
| $\sigma_{av}$ | Area under the curve obtained corresponding to yielding of the plate section |

# CHAPTER 1
# INTRODUCTION

Elastic buckling of plates is an area of research where tremendous work has been done so far. The first reference to buckling arose during the mid-19th century. Walker (1967) conducted a series of tests in University college of London on box beams with variety of tubular shape cross sections. The test results revealed that the failure occurred in most of the cases due to local buckling. But most of these studies considered the applied load as uniformly distributed and with simply supported boundary conditions.

But for structures like supersonic planes where the aerodynamic effects play a significant role, the applied load may not be constant across the loading edge. The above loading condition of varying applied load can be encountered in webs of beam column when subjected to axial compression and bending about the major axis. The case of linearly varying edge loading was first considered independently by Timoshenko (1910) and Boobnov (1914), using approximate methods.

Applications include stiffened plates and thin-walled structural members used in aircraft frame design and the design of the flanges of I-shaped beams that are subjected to major axis bending combined with significant lateral forces (minor axis bending) or torsion (warping normal stresses), which results in a stress gradient across the width of the flange plate This study is an attempt to fill this gap.

A detailed study on post buckling behavior of center line stiffened plates is hence the primary objective of this study. Introduction of rotational stiffness in the center introduces a fifth boundary condition to the plate along with the boundary conditions at the edges. To study the post buckling region for the above mentioned

plate, a clear and thorough knowledge of post buckling analysis of a flat plate which is simply supported on all four boundaries are required.

So in the initial stage of study a flat plate with eccentric edge compressive load was considered. The basic equations governing the elastic behavior of buckled plate given by von Karman was written for the above plate boundary conditions. The Galerkin's series for the stress function as well as the deflection function were derived such that the appropriate boundary conditions are satisfied. Accuracy of the above obtained data is compared with the available literature of Walker (1967).

In the second stage, an initially flat rectangular plate with centerline stiffness was considered for the analysis. A uniaxial eccentric compressive load was applied along the longer dimension. The solution for von Karman differential equation was obtained for the above plate with five boundary conditions. The stress as well as deflection series was formulated and solved. The effect of various parameters were examined in the failure load of the plate. The stress profile across the loaded edge of the plate was carefully examined. Finally an expression for effective width of the plate was proposed in terms of rotational restraint and load eccentricity.

## 1.1 Objectives

- To solve the von Karman Governing differential equation for centerline stiffened plates subjected to linearly varying edge compressive load using Galerkin method.
- Examine the effect of stress gradient ($\alpha$) on stress profile.
- Examine the effect of rotational restraint ($\Gamma$) on stress profile.

- Evaluate the effect of increased number of terms in stress as well as deflection series in the solution.
- Formulation of an expression for effective width of the plate in terms of rotational restraint as well as load eccentricity parameter

## 1.2 Scope and Methodology

Extensive research has been done in rectangular plates subjected to edge compression. But limited research information is available in the case of flat plates subjected to linearly varying edge compressive load with center line, rotationally stiffened. Centerline stiffened plates subjected to eccentric stress distribution is common in aircraft structures and in civil engineering members. The elastic buckling portion of the centerline stiffened plate was already solved by Madhavan and Davison (2005). But post buckling portion for the above plate is yet to be solved which is attempted in this work.

In the initial stage, to check the feasibility of employing Galerkin method for the stated problem, the case of an initially flat rectangular plate was solved. This work was previously carried out by Walker (1967). The initial attempt was to solve the governing differential equation for a flat plate subjected to linearly varying edge compressive load with simply supported boundary conditions.

In the second stage the case of a flat rectangular plate with centerline stiffened boundary conditions was analyzed. The formulation was done in MATLAB. By fixing the value of aspect ratio and load eccentricity parameter, a code was generated. The accuracy of method was checked by increasing the number of terms included in the series. The stress distribution and deflection profile on the plate

surface was carefully examined and the effect of various parameters were considered. Finally expressions for effective width of two halves of the plate was proposed.

To get a more detailed information in the field of plate buckling a number of literatures were reviewed which is given in the succeeding chapter.

# CHAPTER 2
# LITERATURE REVIEW

The first reference to buckling arose during the mid-19$^{th}$ century. **Walker A.C [1]** conducted a series of tests carried out in University college of London on box beams of a variety of tubular shape cross sections associated with a railway bridge project. Test results revealed that the failure occurred in most of the cases due to local buckling. Validation of the experimental data was done by numerically solving the partial differential equation for the plate. The relevant study among this is the study of a rectangular flat plate subjected to linearly varying edge compressive load. The solution of plate buckling problem is obtained using Galerkin method and the results are established by comparing with experimental data. The paper helped in arriving appropriate formulations for the plate with centerline stiffened boundary conditions. Hence the paper was validated with required amount of accuracy.

**K. Bedair, A. N. Sherbourne [2]:** This paper investigated the behavior of plates and stiffener assemblies under uniform compressive stress. A general expression was derived for the prediction of the elastic buckling of the assembly under the general loading condition. The accuracy of the derived expression obtained numerically using Galerkin's method was compared with the other available data. The plate was defined as partially restrained against rotation and energy method was then used to derive approximate expressions for buckling coefficient. Based on the characteristics of the stress field in the buckled plate, analytical expressions for effective width was proposed.

**V. Kalyanaraman, P. Jayabalan [3]:** An analytical procedure was presented in this paper for evaluating the local buckling strength based on which equations for the local buckling stress of unstiffened and unstiffened elements are found out. The Von Karman governing differential equation was solved for the prebuckling portion using Galerkin method and buckling coefficient was obtained. Even though a study was

held with sufficient accuracy in prebuckling portion it was limited to buckling of plates in first mode. The change of buckling mode with aspect ratio also need to be included in the analysis.

**J. C. Eze et. al [4]:** The paper considers the case of a flat rectangular plate with all edges clamped and a uniform compressive load acting along minor axis direction. Galarkin's method was used to solve the Governing partial differential equation for plates given by Kirchhoff (1885). The Governing partial differential equation was suitably modified considering the loading to get the Governing partial differential equation corresponding to the particular case. The required displacement function was obtained in non-dimensional form by applying suitable boundary conditions. An approximate solution for the differential equation of the given problem was assumed satisfying the requirement that the differential equation should be orthogonal to the trial function.

**M Madhavan, J. Davidson [5]:** Elastic buckling problem of an initially perfect flat rectangular plate with centerline stiffened with variable rotational restraint was considered. The equilibrium equation for an elastic rectangular plate given by **von Karman [6]** was solved as an Eigen value problem using Galerkin method. With the increase in rotational stiffness the solution was found to converge with the case of a plate with clamped edges. The variation of buckling coefficient with aspect ratio was presented for varying stress gradient. The pre buckling portion was solved with sufficient amount of accuracy but the post buckling portion of the problem also need to be solved as evaluation of post bucking strength is critical for design. This thesis study is an effort to fill this gap.

**C. W Bert, K Devarakonda [7]:** An analytical solution for buckling of simply supported rectangular plates subjected to sinusoidal in plane compressive stress distribution at each end was presented as a superposed Fourier solution. The resulting in plane stress solution consisted of two normal stresses and a shear stress

which were non-linearly distributed throughout the plane of the plate. Stress distribution showed a decrease in the axial stress as the distance from the loaded edge is increased. The diffusion of stress towards the unbuckled region rapidly rises with the increase in plate aspect ratio.

**M.R. Bambach [8]:** Experimental and numerical study of unstiffened plates and sections was presented. The mechanism that provides post buckling strength was analyzed. It was shown that for unstiffened elements the stress redistribution can occur to an extent that tensile stresses occur in axially compressed slender elements. The unstiffened element was showed to possess significant amount of post buckling strength due to redistribution of longitudinal stresses in the element away from buckled region towards unbuckled portions.

**J. Rhodes [9]:** A brief and superficial study of plate elements subjected to local buckling was considered in the paper. von Karman et.al (1932) started the analysis of thin plates in compression. The concept of effective width was developed by von Karman. **Cox[10]** developed an analysis on compressed plate behavior in which the effect of buckling deflection on plate membrane strains and stresses were developed based on geometric analysis. Cox considered averaged value of membrane strains and neglected in plane effects. The method developed by Cox underestimated the post buckling strength and stiffness and hence called 'lower bound method'.

# CHAPTER 3
# THEORETICAL STUDY

## 3.1 Theory of Plate Buckling

Steel plates are widely used in buildings, bridges, automobiles ships and aircrafts. Unlike beams and columns, which have lengths longer than the other two dimensions and so are modeled as linear members, steel plates have widths comparable to their lengths and so are modeled as two-dimensional plane members. Just as long slender columns undergo instability in the form of buckling, steel plates under membrane compression also tend to buckle out of their plane.
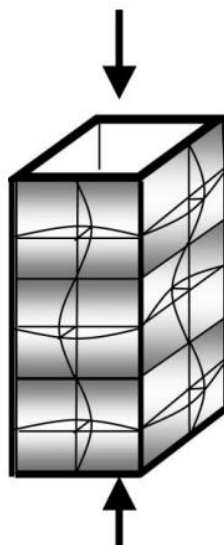


**Fig 3.1. Locally bucked thin wall section**

When a compressed plate buckles, it develops out of plane ripples along its length. The above figure shows a thin walled tubular section where local buckling occurred in all elements. In the elastic range, the buckled portion of the compressed member become incapable of taking further load due to large deflections. But the region close to the unloaded edges can take a major share of the applied compressive load. These regions has post buckling strength as well as stiffness.

The buckled shape of plates depends on the loading and support conditions in both length and width directions. However, unlike columns, plates continue to carry loads even after buckling in a stable manner. The post-buckling behavior of plates is described in terms of both stability and strength and compared with the post-buckling behavior of a column. Noting that the buckling load, $N_{cr}$, is the product of the buckling stress $\sigma_{cr}$ and the thickness, we get the buckling stress as

$$\sigma_{cr} = k\pi^2 E/12(1-\gamma^2)(b/t)^2 \qquad (3.1)$$



**Fig 3.2. Buckling under uniform compression**

As the compressive load on the plate is increased and reaches the critical buckling load, the central part of the plate tends to buckle. For a strip in the transverse direction, it resists the tendency of the strip in the longitudinal direction to deflect out of the plane of the plate.

## 3.2 Post buckling behavior
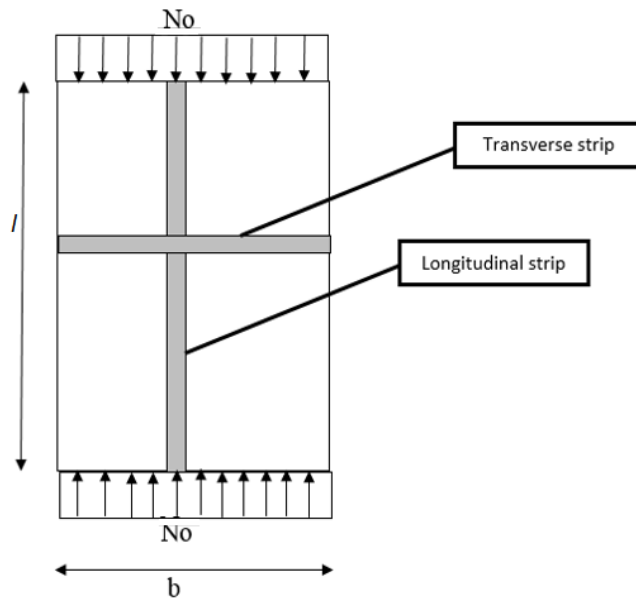
If a longitudinal strip tends to form a single buckle, its curvature will be much less than the curvature of the transverse strip which tries to resist the buckling (l>b). This means that the resistance is greater than the tendency to buckle and the strength corresponding to this mode is very high. Therefore, the plate prefers to buckle such that the curvatures of longitudinal and transverse strips are as equal as possible. This leads to multiple buckles in alternate directions such that the buckles are as square as possible.

When the compressive stress equals the critical buckling stress $\sigma_{cr}$, the central part of the plate buckles. But the edges parallel to the x-axis cannot deflect in the z-direction and so the strips closer to these edges continue to carry the load without any instability. Therefore the stress distribution across the width of the plate in the post-buckling range becomes non-uniform with the outer edges carrying more stress than the inner edges. But transverse strip in the middle surface continue to stretch and support the longitudinal strips. This ensures the stability of the plate in the post-buckling range. When the edge stresses approach and equal the yield stress of the material, the plate deflection would be very large and the plate can be considered to be failed.

## 3.3 Concept of effective width

To calculate the load carrying capacity of the plate in the post-buckling range, the concept of effective width is used. The concept was first proposed by von Karman (1932). He realized that as the plate is loaded beyond its elastic buckling load, the central part deflects thereby shedding the load to the edges. Therefore, the non-uniform stress distribution across the width of the buckled plate, can be replaced by uniform stress blocks of stress equal to that at the edges, over a width of $b_{eff}/2$ on either side where $b_{eff}$ is called the effective width of the plate. This effective width

can be calculated by equating the non-uniform stress blocks and the uniform stress blocks. von Karman effective width equation is given as

$$b_{\text{eff}}/b = \sqrt{(\sigma_{cr}/\sigma_y)} \tag{3.2}$$



**Fig 3.3. Effective width concept**

A modified expression for von Karman's effective width expression was suggested by Winter. When the stress at the outer strips reaches the yield stress, the corresponding effective width can be calculated using Winter's formula

$$b_e/b = \sqrt{(\sigma_{cr}/\sigma_y)} \; (1\text{-}0.25\sqrt{(\sigma_{cr}/\sigma_y)}) \tag{3.3}$$

   Based on effective width the post buckling strength of the plate can be calculated.

## 3.4 Galerkin method
A linear differential operator D is acted on a function 'u' to produce a function 'p',

$$D \, (u(x)) = p(x) \tag{3.4}$$

The function u is approximated by a series of functions $\bar{\upsilon}$, which is a linear combination of basis functions chosen from a linearly independent set. The above concept is expressed as

$$\bar{\upsilon} \cong u = \sum_{i=1}^{n} a_i \varphi_i \qquad (3.5)$$

When the above approximation substituted into the differential operator, D, the result of the operations is different from the value of p(x). The residual or error is obtained as:

$$E(x) = R(x) = D(\bar{\upsilon}(x)) - p(x)) \neq 0. \qquad (3.6)$$

The residual is forced to zero in some average sense over the domain. That is

$$\int R(x) W_i \, dx = 0 \qquad i = 1, 2 \dots n \qquad (3.7)$$

For Galerkin method the weight of the function is taken as

$$W_i = (\partial^2 u / \partial a_i) \qquad (3.8)$$

Here the number of weight functions $W_i$ is exactly equal the number of unknown constants $a_i$ in $\bar{\upsilon}$. The result is a set of n algebraic equations with the unknown constants $a_i$. This method may be viewed as a modification of the Least Squares Method. Rather than using the derivative of the residual with respect to the unknown $a_i$, the derivative of the approximating function is used.

# CHAPTER 4
# NUMERICAL FORMULATION

The numerical formulation for the plate buckling problem is based on the von Karman governing differential equation for an elastic buckled plate. The differential equation is a set of two simultaneous equation which is a function of stress as well as deflection function. A series approximation is made for stress and deflection function based on Galerkin method. Relevant boundary conditions are applied to the stress and deflection functions and finally solved for unknown coefficients.

## 4.1 Assumptions involved

1. Plate material is perfectly elastic, homogenous and isotropic.
2. Thickness of the plate is small compared to other dimensions.
3. Lines perpendicular to middle surface of the plate remain perpendicular after bending.
4. The shear strains $\gamma_{xy}$ and $\gamma_{xz}$ are negligible.
5. The normal stress $\sigma_z$ and its corresponding strain $\varepsilon_z$ are negligible

## 4.2 Formulation of the problem

The fundamental equation governing elastic behavior of a buckled elastic plate is given by von Karman (1910) as,

$$\partial^4 w/\partial x^4 + 2\partial^4 w/\partial x^2\partial y^2 + \partial^4 w/\partial y^4 = t/D \, [\partial^2 F/\partial y^2 \; \partial^2 w/\partial x^2 + \partial^2 F/\partial x^2 \; \partial^2 w/\partial y^2 - 2 \, \partial^2 F/\partial x\partial y \; \partial^2 w/\partial x\partial y] \tag{4.1.a}$$

$$\partial^4 F/\partial x^4 + 2\partial^4 F/\partial x^2\partial y^2 + \partial^4 F/\partial y^4 = E \, [(\partial^2 w/\partial x\partial y)^2 - \partial^2 w/\partial y^2 \; \partial^2 w/\partial x^2] \tag{4.1.b}$$
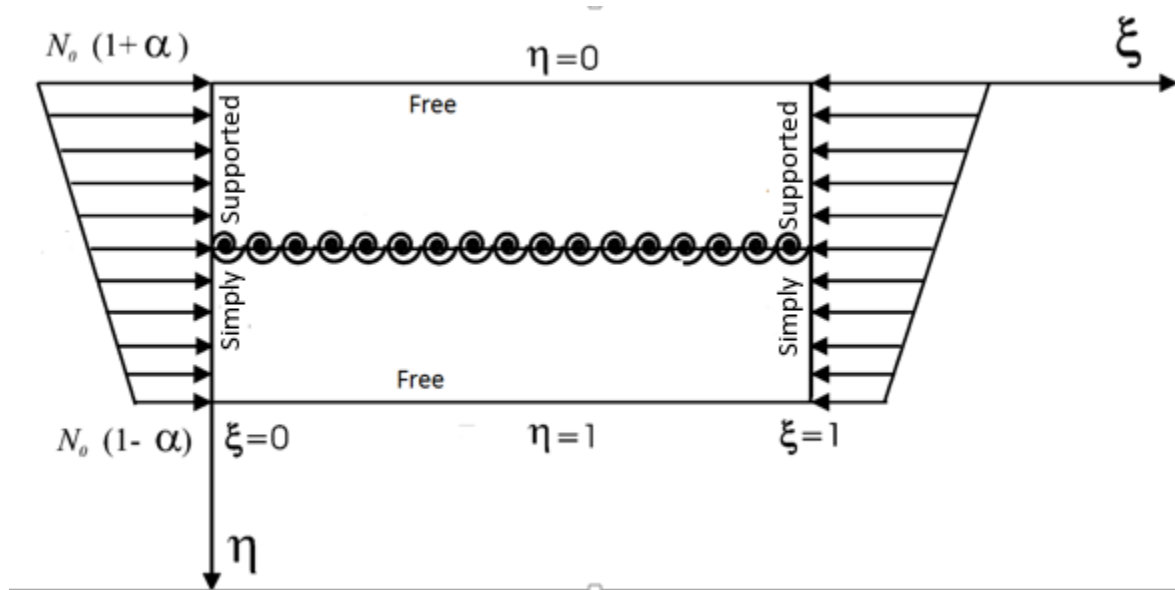
**Fig 4.1. Non dimensional representation of geometry of centerline stiffened plate with uniformly varying load along ξ direction**

The first of these equations, sometimes called the "Compatibility Equation" ensures that in an elastic plate the in-plane and out-of-plane displacements are compatible. The second equation is based on equilibrium principles, and is sometimes termed the "Equilibrium Equation". Exact solution of these equations is only possible for the simplest loading and support conditions, but solutions which are within reasonable accuracy are obtainable for a wide range of problems.

Here x, y, z are the set of Cartesian co-ordinates with xy in the middle surface of the plate in un-deformed condition, w is the normal deflection parallel to z direction in the middle surface of the plate, t is the uniform thickness of the plate, D is the flexural stiffness and F an Airy's stress function which gives direct stresses $\sigma_x$, $\sigma_y$

$$D = Et^3/12(1-\gamma^2) \tag{4.2}$$
$$\sigma_x = \partial^2 F/\partial y^2 \tag{4.3}$$

$$\sigma_y = \partial^2 F/\partial x^2 \tag{4.4}$$

$$\tau_{xy} = -\partial^2 F/\partial x \partial y \tag{4.5}$$

The strain in the middle surface of the plate is given by

$$\varepsilon_x = \partial u/\partial x + \tfrac{1}{2}(\partial w/\partial x)^2 \tag{4.6}$$

$$\varepsilon_y = \partial u/\partial y + \tfrac{1}{2}(\partial w/\partial y)^2 \tag{4.7}$$

$$\gamma_{xy} = \partial u/\partial y + \partial v/\partial x + \partial w/\partial x \; \partial w/\partial y \tag{4.8}$$

Where $\varepsilon_x$ and $\varepsilon_y$ are direct strains parallel to x, y respectively and $\gamma_{xy}$ is the shear strain in the xy plane. For applying Galerkin method in von Karman equation the terms in equations need to be converted to non-dimensional form. Eq. 4.1 can be expressed in non-dimensional form by substituting

*$\xi=x/l,\ \eta=y/b,\ \varphi=l/b,\ \omega=w/t,\ F'=F/Et^2$*

The stresses along the plate surface in non-dimensional form is given by

$$\sigma_\xi = \sigma_x l^2/\varphi^2 E t^2 \tag{4.9}$$

$$\sigma_\eta = \sigma_y l^2/\varphi^2 E t^2 \tag{4.10}$$

$$\tau_{\xi\eta} = \tau_{xy}\, l^2/\varphi^2 E t^2 \tag{4.11}$$

Where *l* is the plate length in x direction and *b* the plate breadth in y direction. Eq.4.1 then becomes

$$1/\varphi^2\, \partial^4\omega/\partial\xi^4 + 2\, \partial^4\omega/\partial\xi^2\partial\eta^2 + \varphi^2\, \partial^4\omega/\partial\eta^4 = 12(1-\gamma^2)\, [\partial^2 F/\partial\eta^2\, \partial^2\omega/\partial\xi^2 + \partial^2 F/\partial x^2\, \partial^2\omega/\partial\eta^2 - 2\partial^2 F/\partial\xi\partial\eta\, \partial^2\omega/\partial\xi\partial\eta] \tag{4.12. a}$$

$$1/\varphi^2\, \partial^4 F/\partial\xi^4 + 2\partial^4 F/\partial\xi^2\partial\eta^2 + \varphi^2\partial^4 F/\partial\eta^4 = [(\partial^2\omega/\partial\xi\partial\eta)^2 - \partial^2\omega/\partial\eta^2\, \partial^2\omega/\partial\xi^2] \tag{4.12. b}$$

An exact solution of the above problem is impossible. Hence an approximate solution for this equation is to be found using Galerkin's method.

## 4.3 Galerkin series derivation for stress function

A rectangular plate which is initially flat is considered in the analysis. The loaded edges are simply supported and the unloaded edges are free. The plate is loaded by a uniformly varying load along two simply supported edges. The formulation in non-dimensional form is used in analysis. At $\xi=0$ and $\xi=1$ the imposed boundary conditions for stress functions are

$$\sigma_{x\,(,x=0,l)}=No/t[(1+\alpha)-2\alpha y/b] \tag{4.13}$$

The above equation in non-dimensional form gives

$$\sigma_{\xi\,(,\xi=0,1)}= \partial^2F'/\partial\eta^2{}_{(\xi=0,1)}=No'[(1+\alpha)\ -2\alpha\eta] \tag{4.14}$$

$$\tau_{\xi\eta\,(,\xi=0,1)}= -\partial^2F'/\partial\xi\partial\eta\,_{(\xi=0,1)}=\ 0$$

Where $N_o'=N_o l^2/\varphi^2 Et^3$

The normal and shear stresses along the unloaded edges are zero.

$$\tau_{\eta\xi\,(\eta\,=0,1)}= \partial^2F'/\partial\xi\partial\eta\,_{(\eta\,=0,1)}=0 \tag{4.15}$$

$$\sigma_{\eta\,(\,\eta\,=0,1)}= \partial^2F'/\partial\xi^2{}_{(\eta\,=0,1)}=0 \tag{4.16}$$

An approximation for the stress function is such that at the loaded edges the stress function returns the assumed value of direct stresses.

$$F'=A\,[(1+\alpha)/2) - \alpha/3\eta]\eta^2+ \sum\sum b_{rs}\,f_r(\xi)g_s(\eta) \tag{4.17}$$

Where A is a constant and $f_r\,(\xi)$ and $g_s\,(\eta)$ are functions of $\xi$ and $\eta$ respectively. Then

$$\partial^2F'/\partial\xi^2= 2A\,[(1+\alpha)/2) - \alpha\eta] + \sum\sum b_{rs}\,\partial^2F'/\partial\eta^2\,f_r(\xi)g_s(\eta) \tag{4.18}$$

At $\xi = (0, 1)$ the stress function is given as

$$\partial^2 F'/\partial\xi^2 = No' [((1+\alpha)/2) - \alpha\eta] \tag{4.19}$$

Hence forcing the series part of equation (4.71) to zero,

$$A [(1+\alpha)/2 - \alpha\eta] = No' [(1+\alpha) - 2\alpha\eta] \tag{4.20}$$

Hence $2A = No'$. Then the assumed form of the stress function can be written as

$$F' = No' [(1+\alpha)/2] - \alpha/3\eta] \eta^2 + \sum_r \sum_s b_{rs} f_r(\xi) g_s(\eta) \tag{4.21}$$

Applying the boundary conditions for stresses to the series part of equation (6) gives

$$\partial^2/\partial\xi^2 [f_r(\xi) g_s(\eta)]_{(\eta=0,1)} = 0 \tag{4.22}$$
$$\partial^2/\partial\eta^2 [f_r(\xi) g_s(\eta)]_{(\xi=0,1)} = 0 \tag{4.23}$$
$$\partial^2/\partial\xi\partial\eta [f_r(\xi) g_s(\eta)]_{(\xi=0,1)} = 0 \tag{4.24}$$
$$\partial^2/\partial\xi\partial\eta [f_r(\xi) g_s(\eta)]_{(\eta=0,1)} = 0 \tag{4.25}$$

Which can be simplified as

$$f_r(\xi)_{(\xi=0,1)} = 0 \tag{4.26}$$
$$d/d\xi [f_r(\xi)]_{(\xi=0,1)} = 0 \tag{4.27}$$

Hence assume $f_r(\xi)$ as

$$f_r(\xi) = \sin^2 r\pi\xi \tag{4.28}$$
$$g_s(\eta)_{(\eta=0,1)} = 0 \tag{4.29}$$
$$d/d\eta [g_s(\eta)]_{(\eta=0,1)} = 0 \tag{4.30}$$

A polynomial function is chosen for $g_s(\eta)$

$$g_s(\eta) = \eta^{s+4} + As\eta^{s+3} + Bs\eta^{s+2} + Cs\eta^{s+2} + Ds\eta^s \tag{4.31}$$

Substituting for $\sigma_\xi$ in equation (4.15) and (4.16) applying boundary conditions, possible forms of solutions of $g_s(\eta)$ are,

$$g_s(\eta)= \eta^{s+4} -2\eta^{s+3} +\eta^{s+2} \tag{4.32}$$

Substituting the obtained values of $f_r(\xi)$ and $g_s(\eta)$ in equation (6) gives the value of F' as

$$F'= No'/2[(1+\alpha/2) + \alpha/3\eta]\ \eta 2 + \sum_{r=1,2}^{T} \sum_{s=0,1}^{U} b_{rs} \sin r\pi\ \xi^2\ [\eta^{s+4} - 2\ \eta^{s+3} + \eta^{s}] \tag{4.33}$$

## 4.4 Galerkin series derivation for deflection function

The loaded edges of the plate are assumed to be simply supported. Hence for loaded edges the boundary conditions expressed in non-dimensional form is

$$M_{\xi(\xi=0,1)}=[\partial^2\omega/\partial\xi^2+\gamma\ \varphi^2\partial^2\omega/\partial\eta^2]_{(\xi=0,1)}\ =0 \tag{4.34}$$

$$\omega_{\xi(\xi=0,1)}=0 \tag{4.35}$$

Unloaded edges are free and hence the boundary conditions are

$$[\partial^2\omega/\partial\eta^2+\gamma\ /\varphi^2\ \partial^2\omega/\partial\xi^2\ ]_{(\eta=0,1)}\ =0 \tag{4.36}$$

$$[\partial^3\omega/\partial\eta^3+(2-\gamma\ )/\varphi^2\ \partial^3\omega/\partial\eta\partial\xi^2\ ]_{(\eta=0,1)}\ =0 \tag{4.37}$$

At $\eta=0.5$ (centerline of the plate), the out of plane deflection and the rotation is arrested. This leads to the boundary conditions

$$[\partial^2\omega/\partial\eta^2+\gamma\ /\varphi^2\ \partial^2\omega/\partial\xi^2\ -\Gamma\partial\omega/\partial\eta\ ]_{(\eta=0.5)}\ =0 \tag{4.38}$$

$$[\omega]_{(\eta=0.5)}= 0 \tag{4.39}$$

Where $\Gamma=r*b/D$ is the non-dimensional form of rotational stiffness.

Now an approximation for $\omega$ satisfying the boundary conditions given by equations 4.34 to 4.39 are to be found out. Assuming $f_m(\xi)$ and $g_m(\eta)$ as two independent functions of $\xi$ and $\eta$ respectively the deflection function is assumed as

$\omega = q_{mn}\, f_m(\xi) g_m(\eta)$

Where $q_{mn}$ are constants. Assumed forms of $f_m(\xi)$ and $g_m(\eta)$ ar

$f_m(\xi) = \sin m\pi\, \xi$ \hspace{4cm} (4.40)

The function $f_m(\xi)$ represents the deflection along loaded edges. Assuming a polynomial function for deflection perpendicular to the loading direction.

$g_m(\eta) = [\, \eta^{n+6} + A_n\eta^{n+5} + B_n\eta^{n+4} + C_n\eta^{n+3} + D_n\eta^{n+2} + E_n\eta^{n+1} + F_n\eta^{n} \,]$ \hspace{1cm} (4.41)

Substituting for $\omega$ gives

$\omega = \sin m\pi\, \xi[\eta^{n+4} + A_n\eta^{n+3} + B_n\eta^{n+2} + C_n\eta^{n+1} + D_n\eta^{n} + E_n\eta^{n+1} + F_n\eta^{n} \,]$ \hspace{0.5cm} (4.42)

Now equations 4.34 to 4.39 are imposed on 4.40 and 4.41. The solution is a set of simultaneous equations. The equations containing the unknowns are written in matrix form to implement in Matlab code.

The above equations are expressed in matrix form as

$$
\begin{bmatrix}
0 & 0 & 0 & 0 & 0 & n(n-1) \\
0 & 0 & 0 & 0 & (n+1)n*(n-1) & 0 \\
\begin{matrix}[4(n+5)(n+4)\\-\beta\gamma-2\Gamma(n+5)]\end{matrix} & \begin{matrix}2[4(n+4)(n+3)\\-\beta\gamma-2\Gamma(n+4)]\end{matrix} & \begin{matrix}4[4(n+3)(n+2)\\-\beta\gamma-2\Gamma(n+3)]\end{matrix} & \begin{matrix}8[4(n+2)(n+1)\\-\beta\gamma-2\Gamma(n+2)]\end{matrix} & \begin{matrix}16[4(n+1)n\\-\beta\gamma-2\Gamma(n+1)]\end{matrix} & \begin{matrix}32[4(n-1)n\\-\beta\gamma-2\Gamma n]\end{matrix} \\
1 & 2 & 4 & 8 & 16 & 32 \\
(n+5)(n+4)-\beta\gamma & (n+4)(n+3)-\beta\gamma & (n+3)(n+2)-\beta\gamma & (n+2)(n+1)-\beta\gamma & (n+1)(n)-\beta\gamma & (n)(n-1)-\beta\gamma \\
\begin{matrix}[(n+5)(n+4)(n+3)\\-(n+5)(2-\gamma)\beta\end{matrix} & \begin{matrix}(n+4)(n+3)(n+2)\\-(n+4)(2-\gamma)\beta\end{matrix} & \begin{matrix}(n+3)(n+2)(n+1)\\-(n+3)(2-\gamma)\beta\end{matrix} & \begin{matrix}(n+2)(n+1)n\\-(n+2)(2-\gamma)\beta\end{matrix} & \begin{matrix}(n+1)(n)(n-1)\\-(n+1)(2-\gamma)\beta\end{matrix} & \begin{matrix}(n)(n-1)(n-2)\\-(n)(2-\gamma)\beta\end{matrix}
\end{bmatrix}
$$

$$
\begin{bmatrix} A_n \\ B_n \\ C_n \\ D_n \\ E_n \\ F_n \end{bmatrix} =
\begin{bmatrix}
0 \\
0 \\
\frac{\beta\gamma}{2} - 2(n+6)(n+5) + \Gamma(n+6) \\
-1/2 \\
\beta\gamma - (n+6)(n+5) \\
(n+6)(2-\gamma)\beta - (n+6)(n+5)(n+4)
\end{bmatrix}
$$

Solving the above equations the coefficients $A_n$, $B_n$, $C_n$, $D_n$, $E_{n\ and}$ $F_n$ are found out. Back substituting the obtained values of coefficients in the series form of deflection function gives the expression for deflection function ($\omega$) as

$$\omega = \sin m\pi\, \xi[\eta^{n+4} + A_n\eta^{n+3} + B_n\eta^{n+2} + C_n\eta^{n+1} + D_n\eta^{n} + E_n\eta^{n+1} + F_n\eta^{n}\,] \qquad (4.43)$$

This series approximation of deflection function is substituted in von Karman governing differential equations along with the series form of stress function and solved for unknown coefficients.

# CHAPTER 5

# FORMULATION OF POSTBUCKLING SOLUTION

## 5.1 Formulation of integral form of von Karman differential equations

An independent solution methodology was developed for solving the von Karman differential equation using Galerkin method. The Galerkin series stress and deflection function were derived in the previous section as

$$F' = No'/2[(1+\alpha/2) + \alpha/3\eta]\,\eta 2 + \sum_{r=1,2}^{T} \sum_{s=0,1}^{U} brs \sin r\pi\,\xi^2\,[\eta^{s+4} - 2\,\eta^{s+3} + \eta^s]$$

(5.1)

$$\omega = \sum_{m=1,2}^{p} \sum_{n=0,1}^{L} \sin m\pi\,\xi\,[\eta^{n+6} + A_n\eta^{n+5} + B_n\eta^{n+4} + C_n\eta^{n+3} + D_n\eta^{n+2} + E_n\eta^{n+1} + F_n\eta^n]$$

(5.2)

Fixing a value for m simplifies the double summation series to a series of single summation. Hence

$$\omega = \sum_{n=0,1}^{L} q_n \sin m\pi\,\xi\,[\eta^{n+6} + A_n\eta^{n+5} + B_n\eta^{n+4} + C_n\eta^{n+3} + D_n\eta^{n+2} + E_n\eta^{n+1} + F_n\eta^n]$$

(5.3)

Generalized term of the stress and deflection function is represented as

$$F_{pq} = b_{pq}\sin^2 r\pi\xi\,[\eta^{s+4} - 2\,\eta^{s+3} + \eta^s]$$

(5.4)

$$\omega_i = q_i\,[\eta^{i+6} + A_i\eta^{i+5} + B_i\eta^{i+4} + C_i\eta^{i+3} + D_i\eta^{i+2} + E_n\eta^{n+1} + F_n\eta^n]$$

(5.5)

The stress function F' is divided as

F'=f1+f2*f3                              where,

f1= No'/2[(1-α/2) + α/3η] η2 $\qquad$ (5.6)

f2=$\sum_{r=1,2}^{T} \sum_{s=0,1}^{U} b_{rs}[\eta^{s+4} - .5\,\eta^{s+2} + 1/16Ds\,\eta^{s}]$ $\qquad$ (5.7)

f3=sin rπ ξ $\qquad$ (5.8)

Applying Galerkin method to the von Karman equation gives

$\sum_{n=0,1}^{L} \sum_{r=1,2}^{T} \sum_{s=0}^{U} \int_{0}^{1}\int_{0}^{1}[1/\varphi^2\ \partial^4 F/\partial\xi^4 + 2\,\partial^4 F/\partial\xi^2\,\partial\eta^2 + \varphi^2\,\partial^4 F/\partial\eta^4 -$

$(\partial^2\omega/\partial\xi\partial\eta)^2 + \partial^2\omega/\partial\eta^2\ \partial^2\omega/\partial\xi^2]dF_{pq}/db_{pq}\,d\eta d\xi=0$ $\qquad$ (5.9)

$\sum_{n=0,1}^{L} \sum_{r=1,2}^{T} \sum_{s=0}^{U} \int_{0}^{1}\int_{0}^{1}[1/\varphi^2\ \partial^4\omega/\partial\xi^4 + 2\,\partial^4\omega/\partial\xi^2\,\partial\eta^2 + \varphi^2\,\partial^4\omega/$

$\partial\eta^4 -12(1-\gamma^2)\ [\partial^2 F/\partial\eta^2\ \partial^2\omega/\partial\xi^2 + \partial^2 F/\partial x^2\ \partial^2\omega/\partial\eta^2 - 2\partial^2 F/\partial\xi\partial\eta\ \partial^2\omega/\partial\xi\partial\eta]$

$d\omega i/dqi\,d\eta d\xi=0$ $\qquad$ (5.10)

## 5.2 Solution of nonlinear simultaneous equations

### 5.2.1 Initializing of constants and values

| Variable used | |
|---|---|
| $q_n$, $q_i$ | Variables in deflection function series |
| $b_{rs}$ | Variable in stress function series |
| T | Maximum Limit of r |
| L | Maximum Limit of n |
| U | Maximum limit of s |
| ξ | Normalized dimensions along x |
| η | Normalized dimensions along y |
| m | Number of half sine waves in the direction of applied load |
| φ | Aspect ratio |
| Γ | Non dimensional rotational restraint |

| Variable | Value |
|---|---|
| Poisson's ratio ($\gamma$) | 0.3 |
| Load eccentricity parameter($\alpha$) | $0 \leq \alpha \leq 1$ |

## 5.2.2. Matrix form of integral expression

By fixing a value of aspect ratio, buckling mode, centerline rotational restraint and by iterating the variables *n,r* and *s* generates a set of non-linear simultaneous equations.

Eqs. 5.9 and 5.10 are expressed in matrix form to simplify the problem.

$$[A]\, b_{rs} = [B]\, [q_i\, q_i] \tag{5.11}$$

$$[C]\, [q_i] = [D]\, [b_{rs}\, q_k] \tag{5.12}$$

Where [A], [B], [C] and [D] represents the matrices whose terms are the outputs of integration. Coefficient matrices $b_{rs}$ and $q_k$ corresponds to the stress and deflection coefficients respectively. The terms inside the double integral (Eqs.5.9 and 5.10) are to be developed as a row matrix. This row matrix is multiplied by the generalized term of stress as well as deflection function which is developed as a column matrix.

## 5.2.3 Generation of matrices

### a) Generation of matrix [A]

The portion of eq. 5.9 which contributes to matrix [A] is

$$[A] = \sum_{n=0,1}^{L} \sum_{r=1,2}^{T} \sum_{s=0}^{U} \int_0^1 \int_0^1 [1/\varphi^2\ \partial^4 F'/\partial\xi^4 + 2\,\partial^4 F'/\partial\xi^2\,\partial\eta^2 + \varphi^2\,\partial^4 F'/\partial\eta^4]\, dF'_{pq}/db_{pq}\, d\xi d\eta \tag{5.12}$$

Where

$F' = No'/2[(1-\alpha/2) + \alpha/3\eta] \eta 2 + \sum_{r=1,2}^{T} \sum_{s=0,1}^{U} brs \sin r\pi \xi^2 [\eta^{s+4} - 2\eta^{s+3} + \eta^s]$

$F_{pq} = b_{pq} brs \sin p\pi\xi^2 [\eta^{s+4} - 2\eta^{s+3} + \eta^s]$

Matrix [A] is a function of F' and $F_{pq}$ only and hence is a series function of 'r' and 's'. Hence 'r' and 's' are iterated from initial points to their maximum values of T and U respectively over eq.5.9 to obtain the matrix [a]. Hence matrix [A] is given as

$$[A]_{TU*TU} = \int_0^1 \int_0^1 [F]_{pq}{}^T [a] d\eta d\xi \tag{5.13}$$

## b) Generation of matrix [B]

The portion of Eq. 5.2 which contributes to matrix [B] is

$$[B] = \sum_{n=0,1}^{L} \sum_{r=1,2}^{T} \sum_{s=0}^{U} \int_0^1 \int_0^1 (\partial^2\omega/\partial\xi\partial\eta)^2 - \partial^2\omega/\partial\eta^2 \, \partial^2\omega/\partial\xi^2] dF_{pq}/$$

$$db_{pq} d\xi d\eta = 0 \tag{5.14}$$

Where,

$\omega = \sin m\pi \xi[\eta^{n+6} + A_n\eta^{n+5} + B_n\eta^{n+4} + C_n\eta^{n+3} + D_n\eta^{n+2} + E_n\eta^{n+1} + F_n\eta^n]$

The unknown coefficients $A_n$, $B_n$, $C_n$, $D_n$, $E_n$ and $F_n$ are found by applying deflection and shear boundary conditions. Iterating the value of *n* from 0 to L over eq.5.9 gives the row matrix [b].Iterating the value of *r* and *s* to T and U gives the column matrix $F_{pq}$.

$$[B]_{TU*LL} = \int_0^1 \int_{-.5}^{.5} [[F]_{pq_{TU*1}}]^T [b]_{1*LL} \, d\eta d\xi \tag{5.15}$$

Stress function F' is given as

$F' = No'/2[(1+\alpha/2) + \alpha/3\eta] \eta 2 + \sum_{r=1,2}^{T} \sum_{s=0,1}^{U} brs \sin r\pi \xi^2 [\eta^{s+4} - 2\eta^{s+3} + \eta^s]$

## c) Generation of matrix [C]

Matrix [C] is obtained as

$[C] = \sum_{n=0,1}^{L} \sum_{r=1,2}^{T} \sum_{s=0}^{U} \int_0^1 \int_0^1 [1/\varphi^2 \, \partial^4\omega/\partial\xi^4 + 2\partial^4\omega/\partial\xi^2 \partial\eta^2 + \varphi^2 \partial^4\omega/\partial\eta^4] d\omega_i/dq_i \, d\xi d\eta - 12(1-\gamma^2) [\partial^2 f1/\partial\eta^2 \, \partial^2\omega/\partial\xi^2 + \partial^2 f1/\partial\xi^2 \, \partial^2\omega/\partial\eta^2 - 2\partial^2 f1/\partial\xi \partial\eta \, \partial^2\omega/\partial\xi \partial\eta] d\omega_i/dq_i \, d\xi d\eta$    (5.16)

Where $\omega_i = q_i [\eta^{n+6} + A_n\eta^{n+5} + B_n\eta^{n+4} + C_n\eta^{n+3} + D_n\eta^{n+2} + E_n\eta^{n+1} + F_n\eta^n]$  (5.17)

Matrix [C] is a series function of $\omega_i$ alone and hence need to be iterated from $n=0$ to L only. Iterating $n$ gives the series form of equation 5.10 as a row vector $[c]_{1L}$
And $[\omega_i]_L$

$[C]_{L*L} = \int_0^1 \int_0^1 \omega_{i_{L*1}}{}^T [c]_{1*L} \, d\eta d\xi$    (5.18)

## d) Generation of matrix [D]

$[D] = \sum_{n=0,1}^{L} \sum_{r=1,2}^{T} \sum_{s=0}^{U} \int_0^1 \int_0^1 12(1-\gamma^2) [\partial^2 f2/\partial\eta^2 \, \partial^2\omega/\partial\xi^2 + \partial^2 f2/\partial\xi^2 \, \partial^2\omega/\partial\eta^2 - 2\partial^2 f2/\partial\xi \partial\eta \, \partial^2\omega/\partial\xi \partial\eta] d\omega_i/dq_i \, d\xi d\eta$    (5.19)

For obtaining matrix [D] we need to iterate the three variable $n$, $r$, $s$ in Eq.5.10

$[D]_{L*TUL} = \int_0^1 \int_0^1 \omega_{i_{L*1}}{}^T [d]_{1*TUL} \, d\eta d\xi$    (5.20)

Eq. 5.9 and 5.10 expressed in matrix form gives

$[A]_{TU*TU} \, b_{rs} = [B]_{TU*LL} \, [q_i^2]$    Hence

$$b_{rs} = [A]_{TU*TU}{}^{-1} [B]_{TU*LL} [q_i q_i] \tag{5.21}$$

Equation 5.2 expressed in matrix form gives

$$[C]_{L*L} [q_i] = [D]_{L*TUL} [b_{rs}q_k] \tag{5.22}$$

Substituting for $b_{rs}$ in equation 5.22 gives

$$[C]_{L*L} [q_i] = [D]_{L*TUL} *([A]_{TU*TU}{}^{-1} [B]_{TU*LL}) *[q_i{}^2] [q_k] \tag{5.23}$$

Hence,

$$[q_i] = ([C]_{L*L}{}^{-1} [D]_{L*TUL}) *([A]_{TU*TU}{}^{-1} [B]_{TU*LL}) [q_i{}^2] [q_k] \tag{5.24}$$

The simultaneous equation which earlier contained $b_{rs}$ and $q_n$ as the unknown coefficients is now reduced to a set of nonlinear equations with a single unknown coefficient $q_n$. The above nonlinear equation is solved using the solver in Matlab. By back substituting the value of $q_n$ in Eq.5.21 gives the value of stress coefficient $b_{rs}$.

# CHAPTER 6
## RESULTS AND DISCUSSION

The nonlinear equation of post buckling was solved using Galerkin method for the plate with centerline rotational stiffeness. The solution was obtained in the form of deflection coefficients using a Matlab solver. Using the available equations which relates stress and deflection coefficients the obtained deflection coefficients were converted to stress coefficients as

$$b_{rs}=[A]_{TU*TU}{}^{-1}[B]_{TU*LL}\ [q_iq_i] \tag{5.20}$$

The stress and deflection coefficients were substituted back into their respective series approximations to obtain the stress and deflection functions.

Fig 6.1 shows the variation of peak deflection with respect to applied compressive load for the plate with centerline rotational restraint. The plate deflection is zero initially till the load reaches the critical buckling load ($N_{cr}$) after which the deflection increases drastically following a parabolic behavior. When $\alpha$ increases, the stress acting on one half side of the plate increases (although the total load acting across the width of the plate remains same) there by decreasing the load at which the plate buckles.

Fig 6.2 shows the variation of transverse peak stress in the plate with respect to applied compressive load. The behavior is linear with a change in slope at the critical buckling point. For small values of applied compression, the effect of $\alpha$ is minimal which increases after the load reaches critical buckling stress. The stress increases with increase in $\alpha$ as the point is located on the highly stressed side.
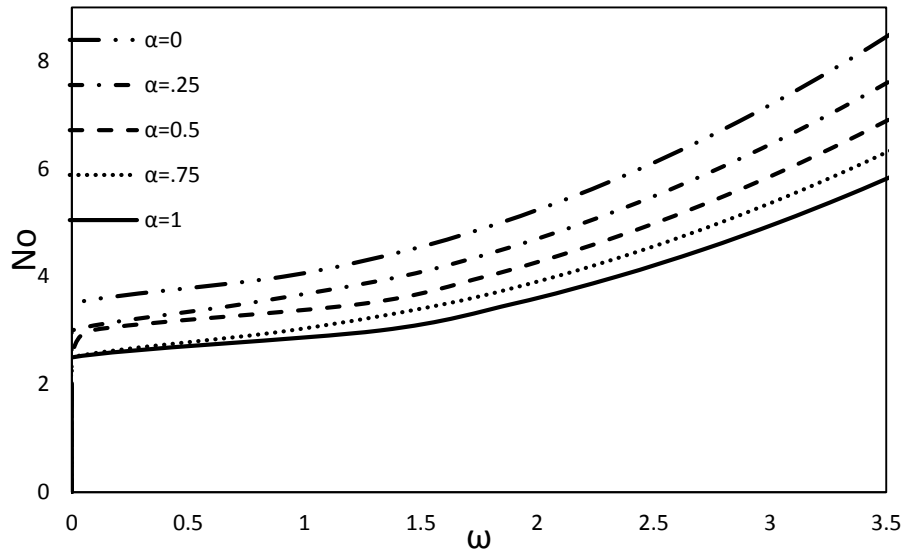
**Fig. 6.1 Load-Deflection plot for varying values of load eccentricity parameter with rotational restraint (Γ)=2,m=2,φ=2**
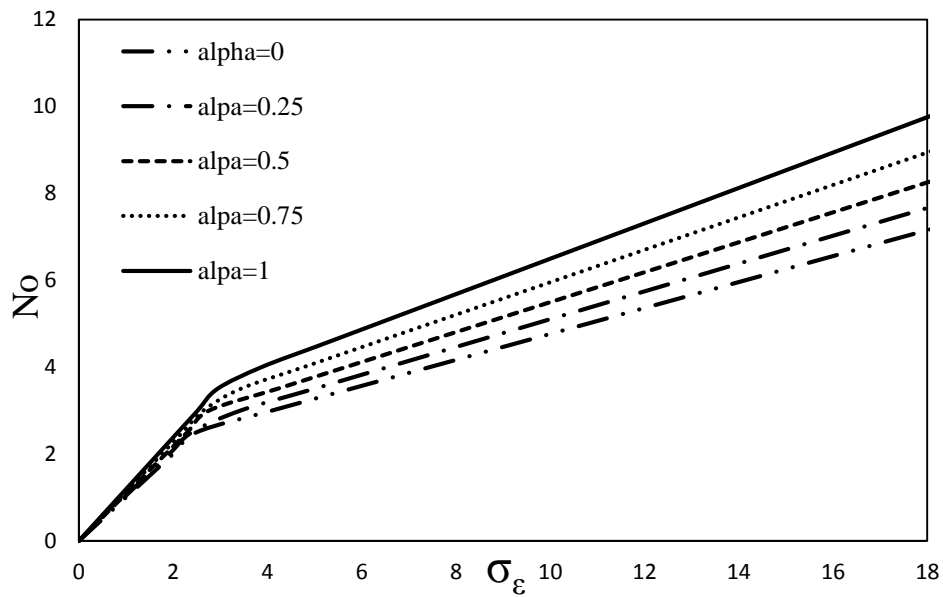


**Fig. 6.2 Stress plot for varying values of load eccentricity parameter with rotational restraint (Γ) =2, m=2, φ=2**

The stress profile with utmost accuracy is always preferred. For increasing the accuracy of stress profile the number of terms included in the series approximation of stress function need to be increased. Also with the increase in number of terms the stress profile should converge.

Thus the optimal number of terms to be included in the series is found out. From Fig 6.3 it is evident that with the increase of number of terms the stress profile converges. There is not much difference between stress profiles corresponding to 6 stress terms ($b_{rs}$) and 12 stress terms. Therefore, in a present research the results are tabulated for 6 stress terms.
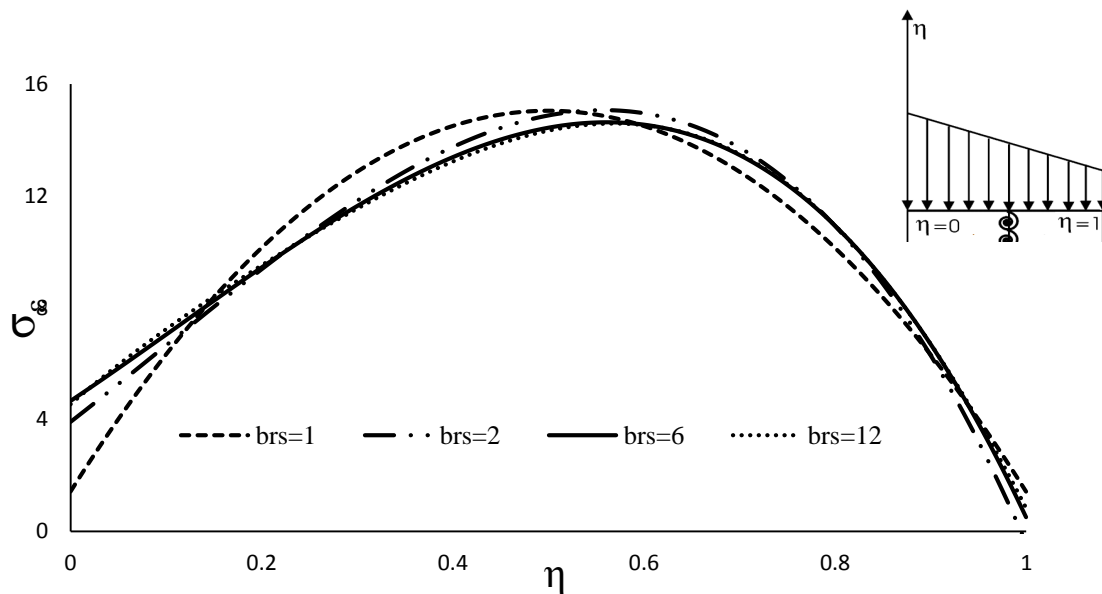
**Fig.6.3 Convergence of stress profile for increased number of terms included in series approximation with m=2, φ=2, α=0.25, Ɛ=0.5, Γ=2**

Fig 6.4 shows the stress profile variation with respect to load eccentricity parameter. The variation of stress across the plate section is following a nonlinear behavior. As the edges η=0 and η=1 are free the stress distribution is concentrated

more towards the edge which is supported, i.e., towards the centerline. For the case of $\alpha=0$, the stress profile is clearly symmetric with respect to the center. But with the increase in $\alpha$, the distribution changes such that the curve shifts towards the highly compressed half. This is attributed to the variation in load distribution which changes from a uniform compression to a triangular load with the increase in $\alpha$ from 0 to 1.
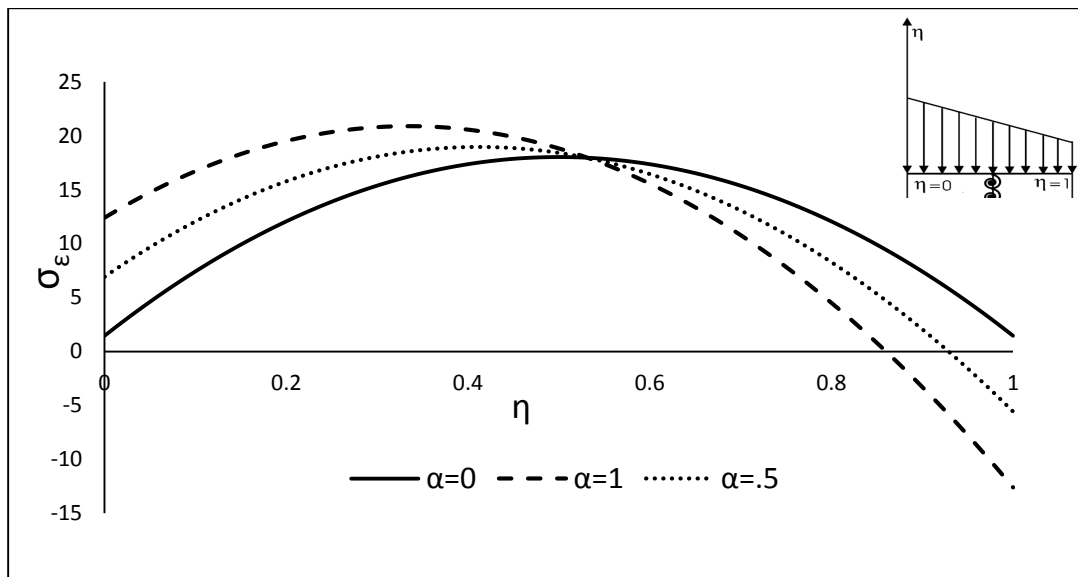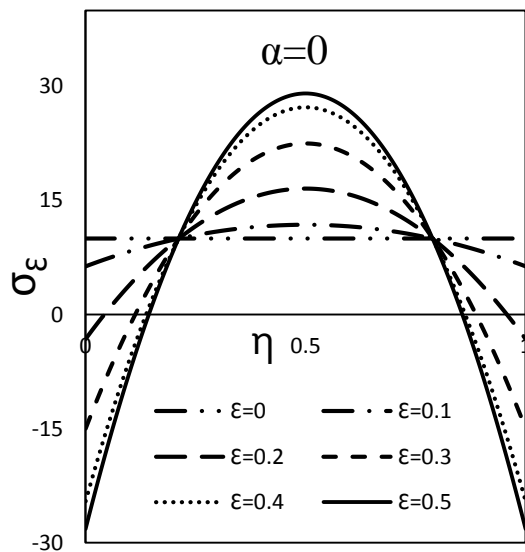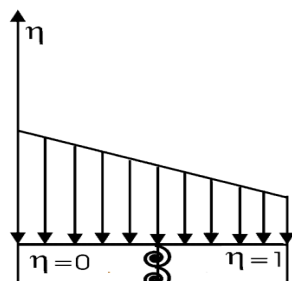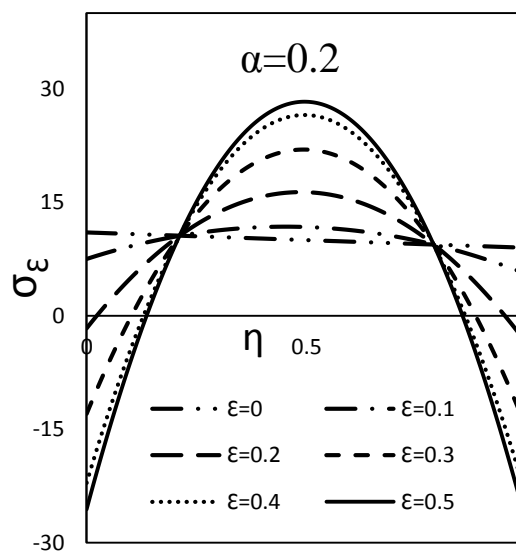


**Fig.6.4 Stress profile across the plate for varying values of load eccentricity parameter with m=2, φ=2, Ɛ=0.5, No=20, Γ=2**
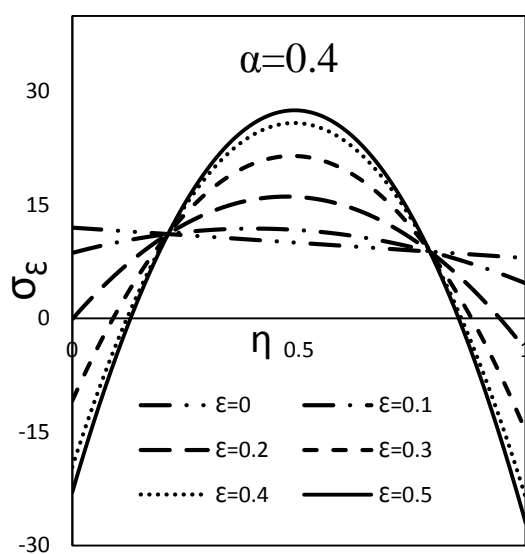
Fig 6.5 shows the stress profile across the width of the plate at different plate sections perpendicular to the loading direction for varying values of $\alpha$. When plate section tends towards the center, the stress profile changes to more nonlinear behavior. According to the concept of post buckling, the stresses shifts from the unsupported edge towards the supported edge in the post buckling range. This is clearly visible at sections which are in the proximity of centerline of the plate. With increase in $\alpha$, eccentricity in the loading increases. The shift of stress profile towards the highly compressed side of the plate is a direct consequence of this which is evident from Fig 6.4 (a) to (f).
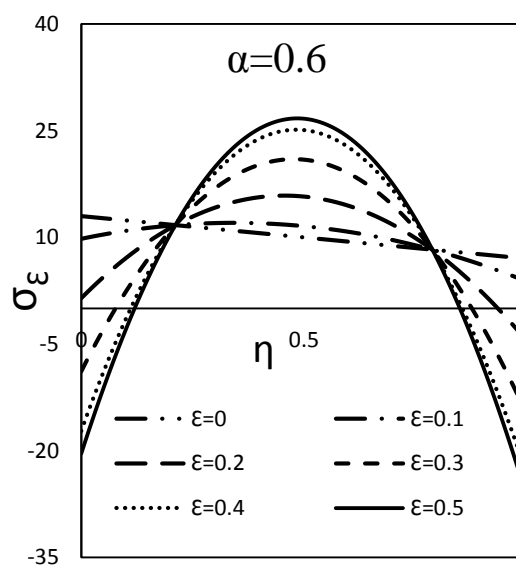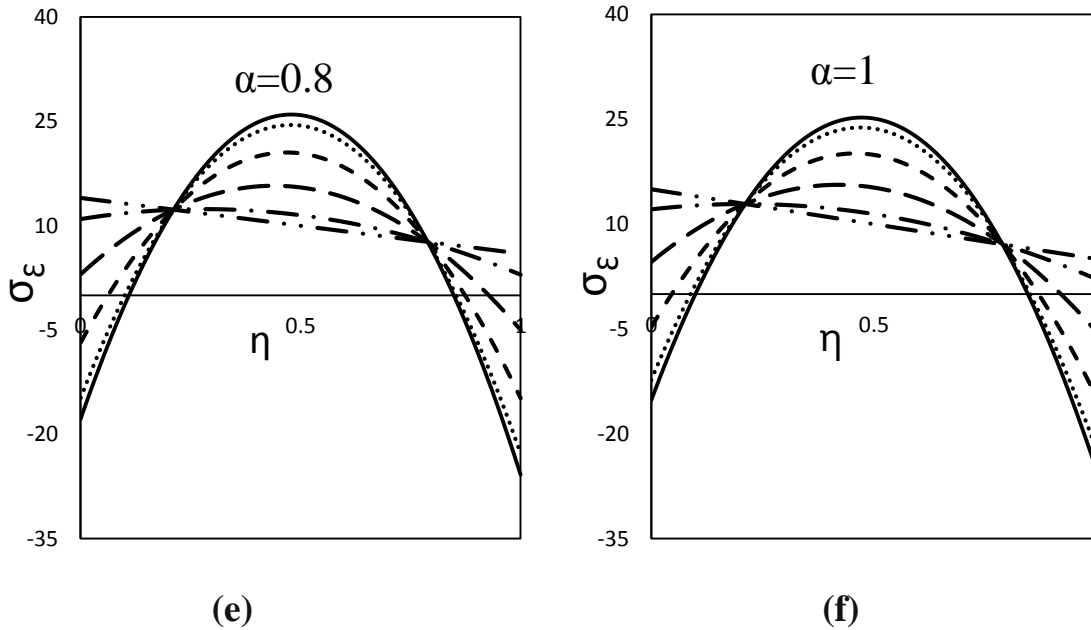
η

η = 0     η = 1

**α=0**

30

15

$\sigma_\varepsilon$

0

η  0.5

-15

-30

··· ε=0          ···· ε=0.1
—— ε=0.2        ——— ε=0.3
········ ε=0.4   ——— ε=0.5

**(a)**

**α=0.2**

30

15

$\sigma_\varepsilon$

0

η  0.5

-15

-30

··· ε=0          ···· ε=0.1
—— ε=0.2        ——— ε=0.3
········ ε=0.4   ——— ε=0.5

**(b)**

**α=0.4**

30

15

$\sigma_\varepsilon$

0

η  0.5

-15

-30

··· ε=0          ···· ε=0.1
—— ε=0.2        ——— ε=0.3
········ ε=0.4   ——— ε=0.5

**(c)**

40

**α=0.6**

25

10

$\sigma_\varepsilon$

-5

η  0.5

-20

-35

··· ε=0          ···· ε=0.1
—— ε=0.2        ——— ε=0.3
········ ε=0.4   ——— ε=0.5

**(d)**

**Fig.6.5 Variation of transverse stress for different cross sections along the plate axis for varying values of α for m=2, φ=2 and Γ=2**

Fig 6.6 depicts the effect of centerline rotational restraint on stress profile of the plate. With the increase in rotational restraint at the plate center, the stiffness increases and the plate reaches a condition where the two halves of the plate show independent behavior. As a result the stresses at the center gets redistributed towards the unloaded edges. For the case of uniform compression there is hardly any effect of rotational restraint. As the load eccentricity parameter increases from α=0 to α=1 (fig (a) to (f)), the effect of rotational stiffness is more significant.

(a)

(b)

(c)
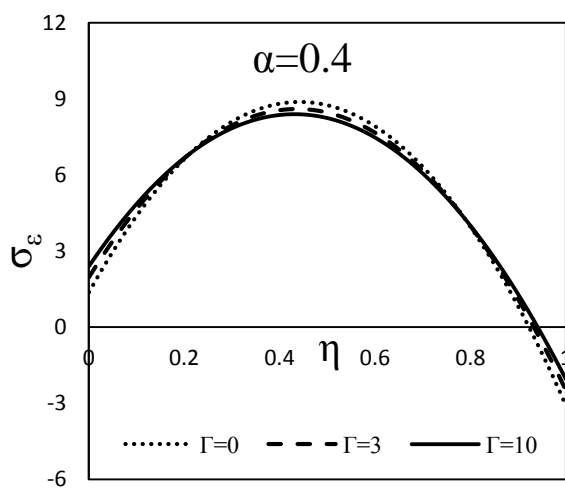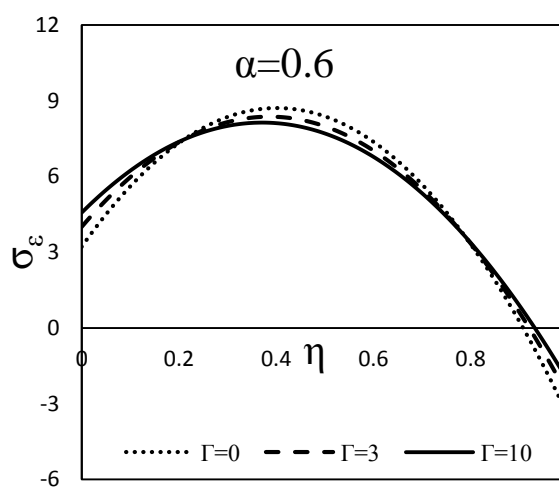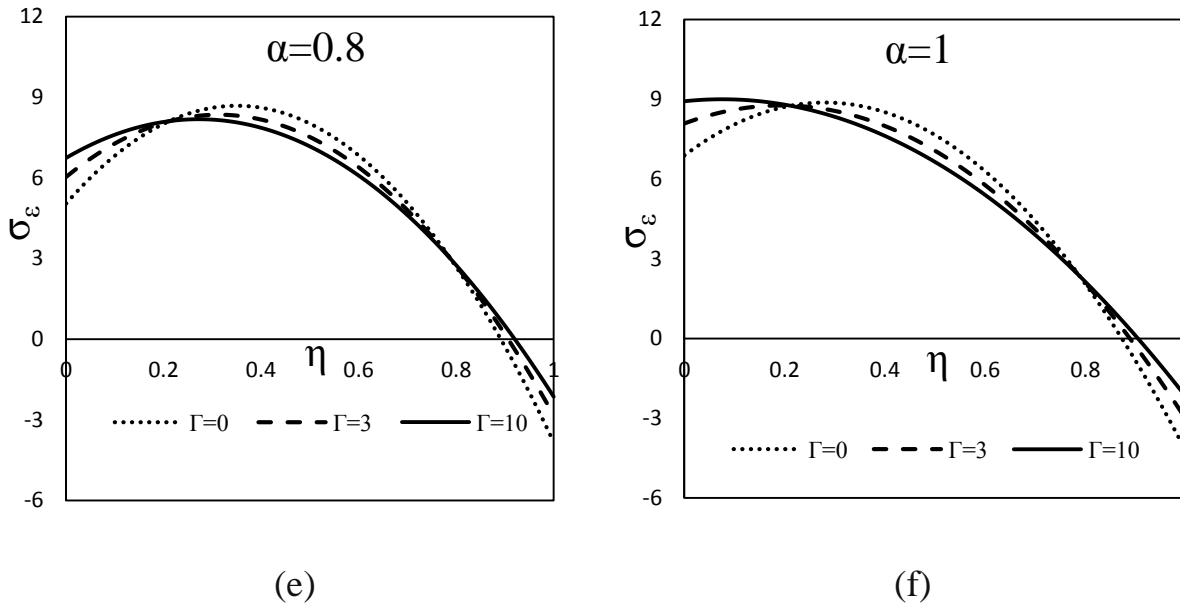
(d)

(e)                       (f)
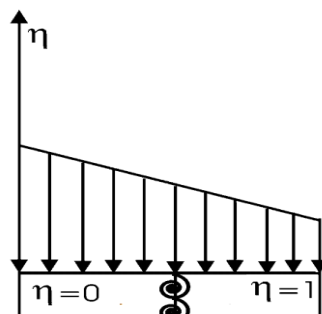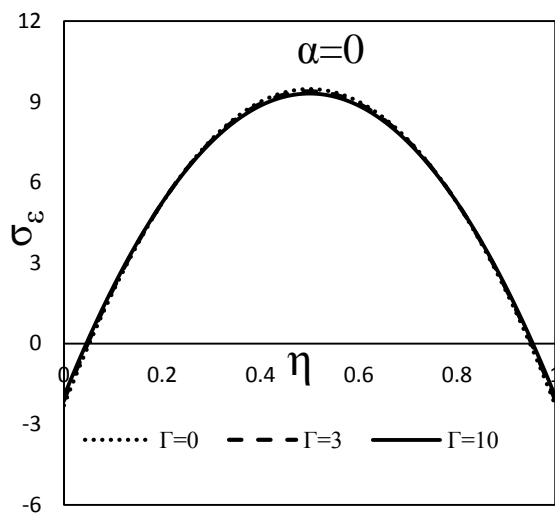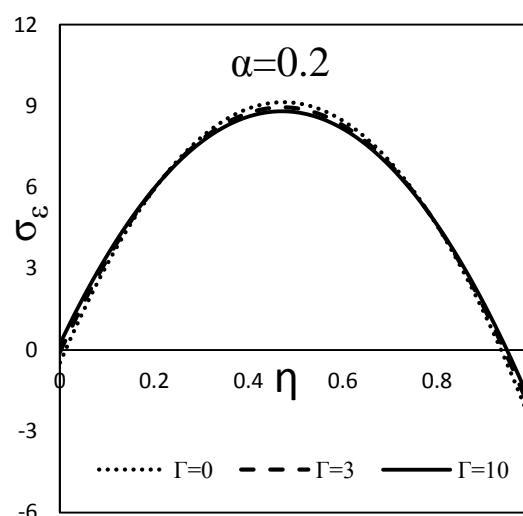
**Fig.6.6 Stress profile across the plate for varying values of centerline rotational restraint for varying load eccentricity parameter, (α) with m=2, φ=2**

Fig 6.7 shows the variation of plate deflection across the width of the plate at different sections in the transverse direction for varying values of α. The deflection of plate initially increases from zero reaches a maximum and again goes back to zero at the center. The deflection profile of the plate is symmetric with respect to the longitudinal axis of the plate but with opposite signs for α=0 but becomes eccentric with increase in α as can be seen in Fig. 6.7 (a) – 6.7(f). This is because due to eccentric loading on one half of the plate, the heavily compressed side results in excessive deflection.

(a)                                          (b)
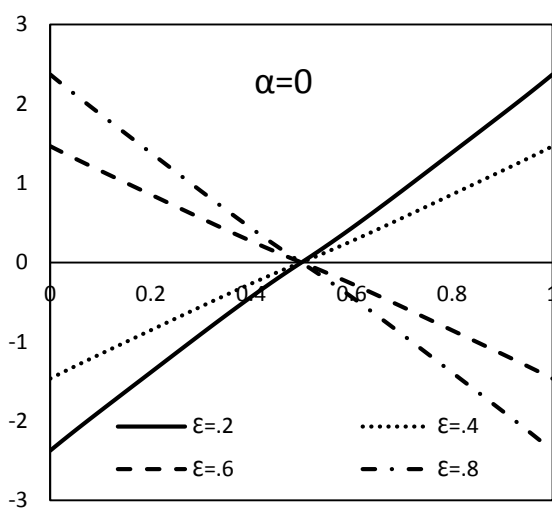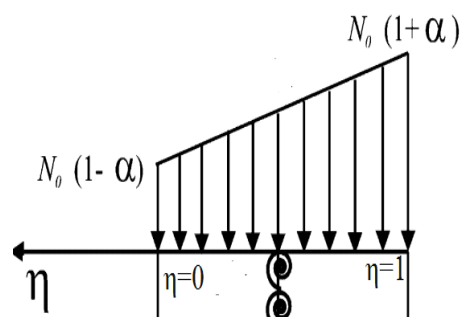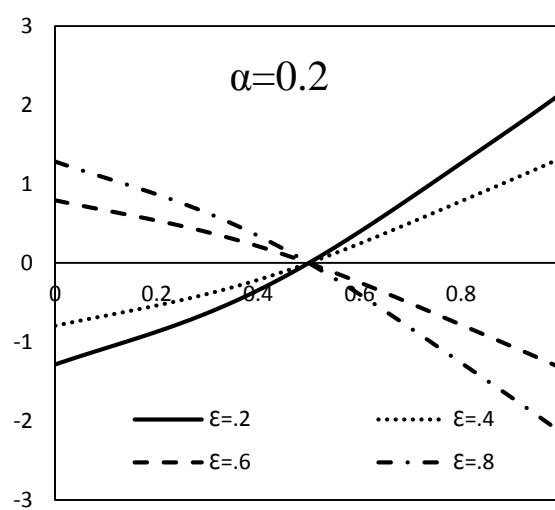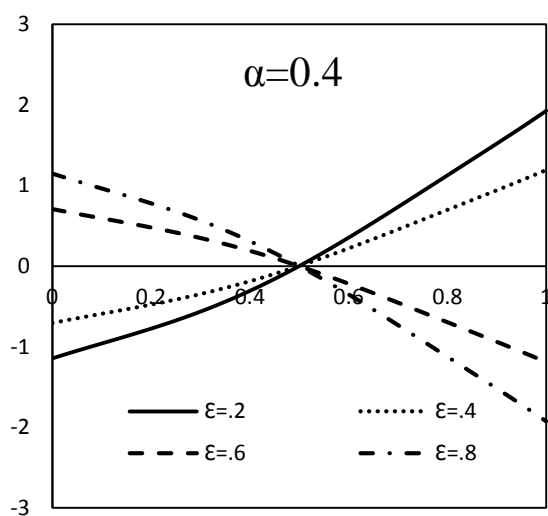
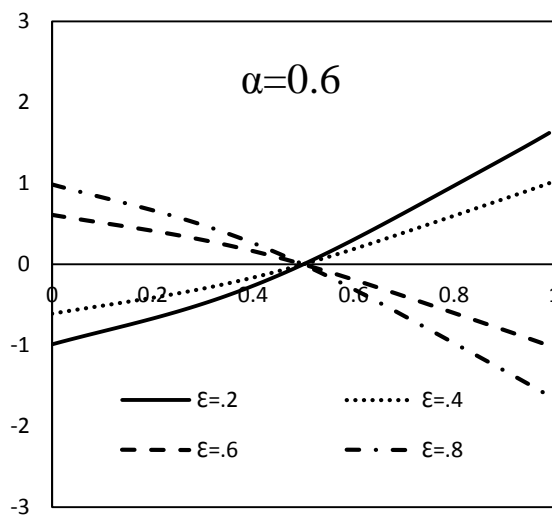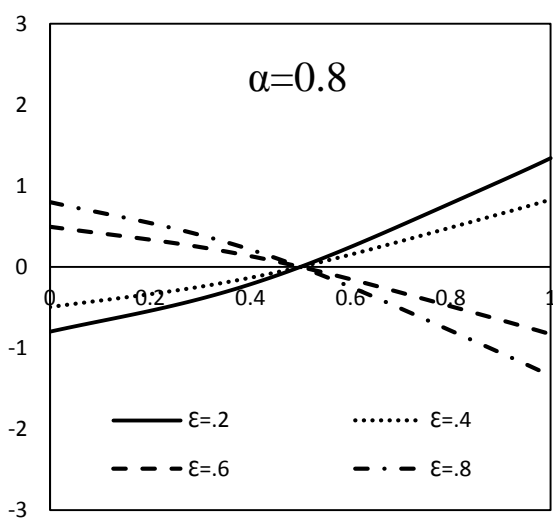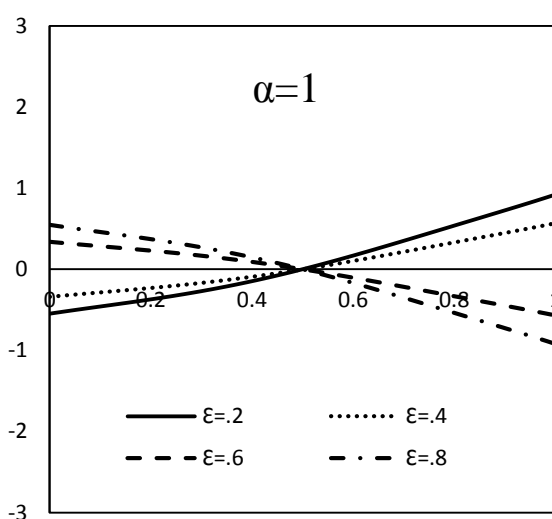**Fig.6.7 Variation of deflection for different cross sections along the plate axis for varying values of α with φ =2, m=2 and Γ=2**

## 6.1 Calculation of effective width

The objective of current work is to deduce an expression for effective width of a centerline stiffened plate subjected to uniaxial eccentric compression. As the load is eccentric, the effective width for two halves of the plate cannot be same. Hence, separate effective width expressions are proposed for two halves of the plate in terms of α and Γ. The same method is adopted for deriving the relation between $\sigma_{cr}$, α and Γ.

## 6.2 Algorithm for relation between α, Γ and σ$_{av}$

The final objective of work was to deduce an expression for effective width of a plate, centerline stiffened, subjected to uniaxial eccentric compression. As the load is eccentric, the effective width for two halves of the plate cannot be same. Hence separate effective width expressions were proposed for two halves of the plate in terms of α and Γ. The same method was adopted for deriving the relation between σ$_{cr}$, Γ and α so that the plate effective width can be expressed in terms of σ$_{cr}$ which is a more critical parameter.

Fix the values m, φ, b$_{rs}$ and q

↓

α is varied from 0 to 1.

↓

For each value of α, Γ is
varied from 0 to 10

↓

For each combination of α and Γ the
von Karman differential equation is
solved

↓

Obtain stress distribution across the plate section
when the extreme fiber reaches yield section

↓

Divide the area under the curve into two
halves along the centerline of the plate and
calculate each area

↓

The input and output variables are stored in
the form of a matrix in spreadsheet

↓

An expression is developed for the relation between
α, Γ, and σ$_{av}$ separately for two halves of the plate
using curve fitting tool in MATLAB

To derive the relation between α, Γ and σ$_{av}$, the stress across the loading direction of the plate is plotted. For increase in value of α, the location of peak stress in the plate shifts towards the highly stressed side of the plate from plate center. By

plotting the stress profile in $\varepsilon$ as well as $\eta$ direction, the section at which stress reaches its yield first is identified. Thus for each value of $\alpha$, the section at which stress reaches it maximum is identified and load is incremented till the peak value of stress reaches its yield. The stress profile corresponding to yielding of section is identified and the area under the profile is calculated for two halves of the plate as $\sigma_{av1}$ and $\sigma_{av2}$.
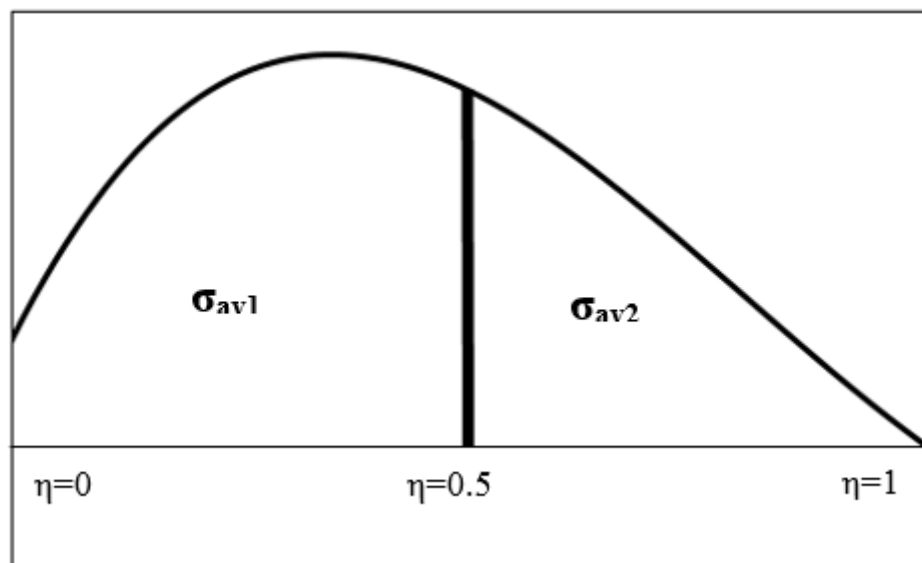


**Fig.6.9 Stress profile across the section of the plate perpendicular to loading direction with area under the curve $\sigma_{av1}$ and $\sigma_{av2}$ with profile shifted towards highly stressed side**

Fig 6.10 shows the variation of $\Gamma$ and $\sigma_{av}$ for varying values of $\alpha$. From plot it is evident that the effect of $\Gamma$ in $\sigma_{av}$ is negligible. But the parameter $\alpha$ is found to make significant effect on $\sigma_{av}$. Fig 6.10 (a), which corresponds to the highly stressed side of the plate, the stresses are significantly higher when compared to the least compressed half, Fig 6.10(b). Hence the effective width corresponding to the highly compressed half should be higher.
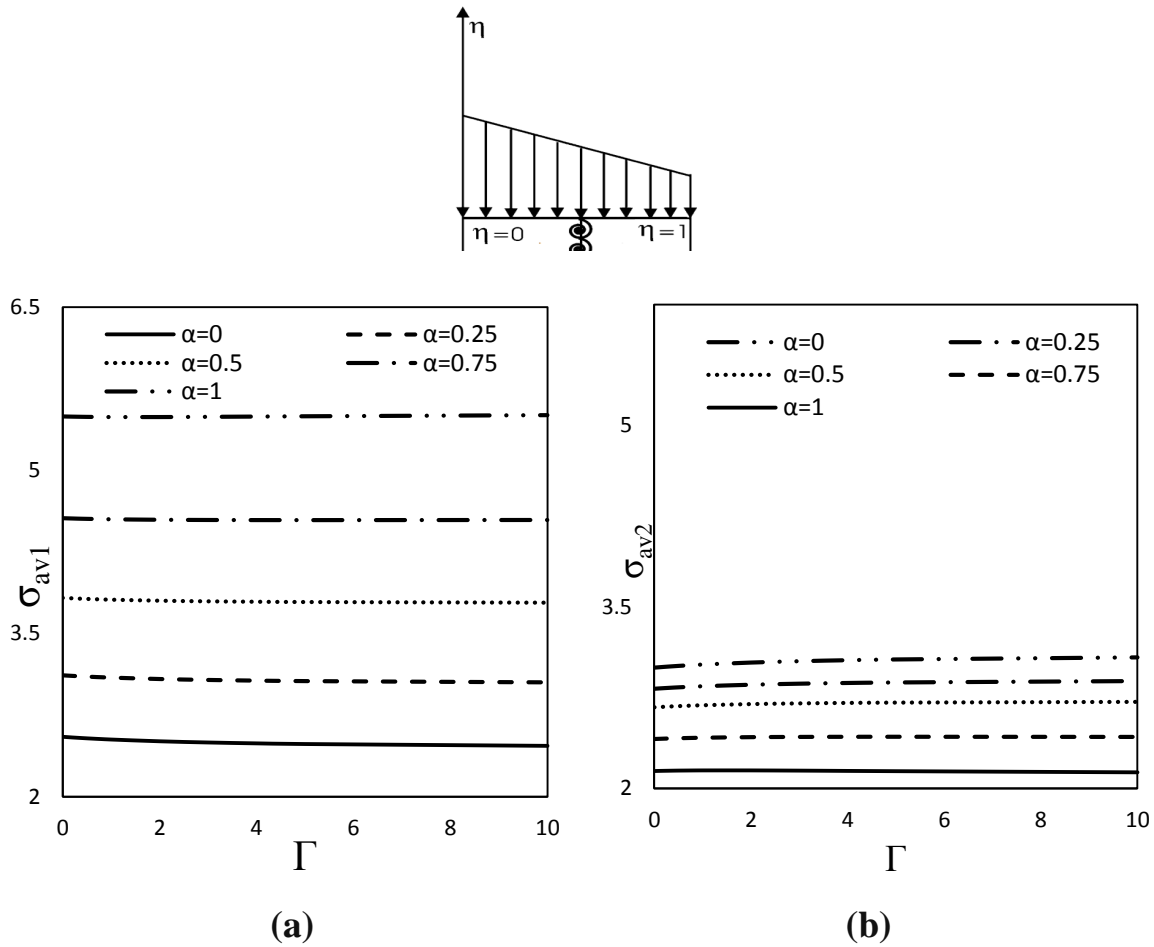
**Fig.6.10 Variation of $\Gamma$ in relation to $\sigma_{av1}$ and $\sigma_{av2}$ for different values of $\alpha$**

Curve fitting tool of MATAB (cftool) is used for deducting the expressions. A second degree polynomial is obtained as the solution with Sum of Square due to Error (SSE) value 0.0176 and R-square value 0.998. The obtained expressions are given as

$$\sigma_{av1}= [2.2+1.79\alpha-.012\Gamma-0.76\alpha^2] = g_1\ (\alpha,\ \Gamma) \qquad (6.1)$$

$$\sigma_{av2}= [2.6-.45\alpha-0.011\Gamma+0.29\alpha^2] = g_2\ (\alpha,\ \Gamma) \qquad (6.2)$$

In the next stage a relation is developed between $\sigma_{cr}$, $\alpha$ and $\Gamma$ following the same solution strategy. A linear polynomial function is obtained as the solution with SSE value 0.0421 and R-square value 0.957.

$$\sigma_{cr} = 2.55+0.423\alpha+0.067\alpha\Gamma+0.55\alpha^2 \qquad (6.3)$$

$$\Gamma=14.92\sigma_{cr}-(38+6.31\alpha+8.2\alpha^2)/\alpha=g_3(\alpha, \sigma_{cr}) \qquad (6.4)$$

Substitute for $\Gamma$ in Eq.6.1 and Eq.6.2 gives

$$\sigma_{av1}= [2.2+1.79\alpha-.012g_3(\alpha, \sigma_{cr}) -0.76\alpha^2] \qquad (6.5)$$

$$\sigma_{av2}= [2.6-.45\alpha-0.011g_3(\alpha, \sigma_{cr}) +0.29\alpha^2] \qquad (6.6)$$

In the post buckling range

$$b_{e1}\sigma_y=\sigma_{av1}b/2 \qquad (6.7)$$

$$b_{e1}= \sigma_{av1}b/2\sigma_y \qquad (6.8)$$

Where $b_{e1}$ is the effective width corresponding to $\sigma_{av1,}$ b the width of the plate and $\sigma_y$ the yield stress of the plate material. The expression for effective width of centerline stiffened plate is obtained as

$$b_{e1}= [2.116+1.72\alpha-.011g_3-0.728\alpha^2]b/2\sigma_y \qquad (6.9)$$

$$b_{e2} = [2.6-.45\alpha-0.011g_3+0.29\alpha^2]b/2\sigma_y \qquad (6.10)$$

## 6.3 Numerical examples to demonstrate the applicability of the proposed equation.

Validation of the obtained equations are done by comparing the results with the theoretical data. For this the section at which yielding initiate's is identified and stress profile across the section is plotted. The load at which section starts yielding

is applied. Area under the curve is found by integration and is compared with the area obtained using the formula

**Example 1**

$\alpha = 0.5$

$\Gamma = 2$

$\gamma = 0.3$

$b_{e1} = \sigma_{av1} b/2\sigma_y$

$b_{e2} = \sigma_{av2} b/2\sigma_y$

$\sigma_{cr}$ obtained from buckling curve of the plate=3

Area under the curve corresponding to $\sigma_y$ for each half of the plate was found out by integration.

$\sigma_{t1} = 3.27$   (non-dimensional form)

$\sigma_{t2} = 2.4$    (non-dimensional form)

Hence

$b_{e1} = 3.27 b/2\sigma_y$

$b_{e2} = 2.4 b/2\sigma_y$

Now using the derived equation for effective width of the plate,

$\sigma_{cr} = 2.55 + 0.423\alpha + 0.067\alpha\Gamma + 0.55\alpha^2 = 3$       (critical buckling stress)


$b_{e1} = [2.116 + 1.72\alpha - .011 f_3 + 0.728\alpha^2] b/2\sigma_y]$                                          (6.9)

$b_{e2} = [2.6 - .45\alpha - 0.011 \Gamma + 0.29\alpha^2] b/2\sigma_y$                                          (6.10)


$b_{e1} = [2.116 + 1.72*.5 + .011*2 - 0.728*.5^2] b/2\sigma_y = 3.14 b/2\sigma_y$

$b_{e2} = [2.6 - .45\alpha - 0.011 \Gamma + 0.29\alpha^2] b/2\sigma_y = 2.42 b/2\sigma_y$

Percentage error in estimation of $b_{e1} = 3.9\%$

Percentage error in estimation of $b_{e2} = 0.8\%$

Percentage error in estimation of $\sigma_{cr}$=0

**Example 2**

$\alpha$=0.25

$\Gamma$=1

$\gamma$= 0.3

$b_{e1}=\sigma_{av1}b/2\sigma_y$

$b_{e2}=\sigma_{av2}b/2\sigma_y$

Area under the curve obtained by integration,

$\sigma_{t1}$= 2.73   (non-dimensional form)

$\sigma_{t2}$= 2.52    (non-dimensional form)

$\sigma_{cr}$ obtained from buckling curve of the plate =2.79

Hence

$b_{e1}$=2.73b/2$\sigma_y$

$b_{e2}$=2.52b/2$\sigma_y$

Now using the derived equation

$\sigma_{cr}$ = 2.55+0.423$\alpha$+0.067$\alpha\Gamma$+0.55$\alpha^2$=2.81          (critical buckling stress)

$b_{e1}$= [2.116+1.72$\alpha$-.011$f_3$+0.728$\alpha^2$]b/2$\sigma_y$]                              (6.9)

$b_{e2}$ = [2.6-.45$\alpha$-0.011 $\Gamma$ +0.29$\alpha^2$]b/2$\sigma_y$                              (6.10)

$b_{e1}$=[2.116+1.72*.25+.011*1-0.728*.25$^2$]b/2$\sigma_y$ =2.51b/2$\sigma_y$

$b_{e2}$=[2.6-.45$\alpha$-0.011 $\Gamma$ +0.29$\alpha^2$]b/2$\sigma_y$=2.49b/2$\sigma_y$

Percentage error in estimation of $b_{e1}$=8%

Percentage error in estimation of $b_{e2}$=1.19%

Percentage error in estimation of $\sigma_{cr}$=0.7%

# CHAPTER 7
# CONCLUSION

In the preliminary stage an initially flat rectangular plate with simply supported boundary condition was considered in the analysis which was subjected to a linearly varying edge compressive load. The governing differential equation for a buckled elastic pate given by von Karman was solved using Galerkin method for post buckling region. The solution was obtained by converting the equation containing stress and deflection coefficients to a single variable equation of deflection coefficients. The solution obtained using Matlab solver was found to be within reasonable limits when compared with the available data given by Walker (1967).

Hence the case of a centerline stiffened plate with unloaded edges free was considered in the analysis. Stress and deflection functions were developed using available boundary conditions and applied to the von Karman differential equation. Galerkin method is used to solve the partial differential equation.

With the increase in number of terms the stress profile was found to converge. Hence the number of terms to be included in the stress as well as deflection series was fixed. The shift of stress from the unsupported edge towards the supported edge in the post buckling range was clearly visible at sections which are in the proximity of centerline of the plate.

Plate rotational restraint at was found to affect the stress distribution. With the increase in plate rotational restraint, stiffness increases and the plate reached a condition where the two halves of the plate showed independent behavior. As a result, the stresses at the center gets distributed towards the unloaded edges. Finally expressions for effective width of the plate was proposed for the initially flat

centerline stiffened plate. As the applied load at two halves of the plate was different, separate expressions were derived for the two halves of the plate.

## FUTURE WORK

- The study can be extended for the analysis of post buckling behavior for the case of a flat plate with eccentric stiffness.
- Inclusion of plate imperfections for the case of centerline stiffened plate.

## REFERENCE

Bambach M.R. (2006). "Local buckling and post-local buckling redistribution of stress in slender plates and sections" Thin-Walled Structures 44 (2006) 1118–1128.

Bedair, O. K., and Sherbourne, A. N. (1995). "Plate/Stiffener Assemblies under Non Uniform Edge Compression." Journal of Structural Engineering, ASCE, 121 (11), 1603-1612.

Boobnov I.G., .(1914)."On thr stresses in ship's bottom plating due to water pressure". vol.2, p.515, St. Petersburg

Bulson, P. S. (1969). The Stability of Flat Plates, American Elsevier Publishing Company, Inc., NY.

Chajes, A. (1974). Principles of Structural Stability Theory, Prentice-Hall, Englewood.

Charles W. Bert, Krishna K. Devarakonda (2003) "Buckling of rectangular plates subjected to nonlinearly distributed in-plane loading" International Journal of Solids and Structures 40 (2003) 4097–4106

J. Rhodes. (2003). "Some observations on the post-buckling behavior of thin plates and thin-walled members" Thin-Walled Structures 41 (2003) 207–226.

Madhavan. M and Davidson. J.S (2005) "Buckling of centerline-stiffened plates subjected to uniaxial eccentric compression" Thin-Walled Structures 43 (2005) 1264–1276.

V. Kalyanaraman and P. Jayabalan. (1994) "Local buckling of stiffened and unstiffened elements under non uniform compression" Twelfth International Specialty Conference on Cold-Formed Steel Structures St. Louis, Missouri, U.S.A., October 18-19, 1994

Walker, A. C. (1967). "Flat Rectangular Plates Subjected to Linearly Varying Edge Compressive Loading." Thin Walled Structures (Ed. A. H. Chilver), 208-247, John Wiley and Sons.

# APPENDIX

Numerical formulation as well as solution for the case of a flat plate simply supported on all four edges is attempted in the first stage of study. The formulation is an implementation of the work done by A.C. Walker (1967). The numerical formulation for the plate buckling problem is based on the von Karman Governing differential equation for an elastic buckled plate. The differential equation is a set of two simultaneous equation which is a function of stress as well as deflection function. A series approximation is made for stress and deflection function based on Galerkin method. Relevant boundary conditions are applied to the stress and deflection functions and finally solved for unknown coefficients.

## A.1 Formulation of the problem

The fundamental equation governing elastic behavior of a buckled elastic plate is given by von Karman (1910) as,

$$\partial^4 w/\partial x^4 + 2\partial^4 w/\partial x^2 \partial y^2 + \partial^4 w/\partial y^4 = t/D \, [\partial^2 F/\partial y^2 \; \partial^2 w/\partial x^2 + \partial^2 F/\partial x^2 \; \partial^2 w/\partial y^2 - 2 \, \partial^2 F/\partial x \partial y \; \partial^2 w/\partial x \partial y]$$

(i.a)

$$\partial^4 F/\partial x^4 + 2\partial^4 F/\partial x^2 \partial y^2 + \partial^4 F/\partial y^4 = E \, [(\partial^2 w/\partial x \partial y)^2 - \partial^2 w/\partial y^2 \; \partial^2 w/\partial x^2]$$
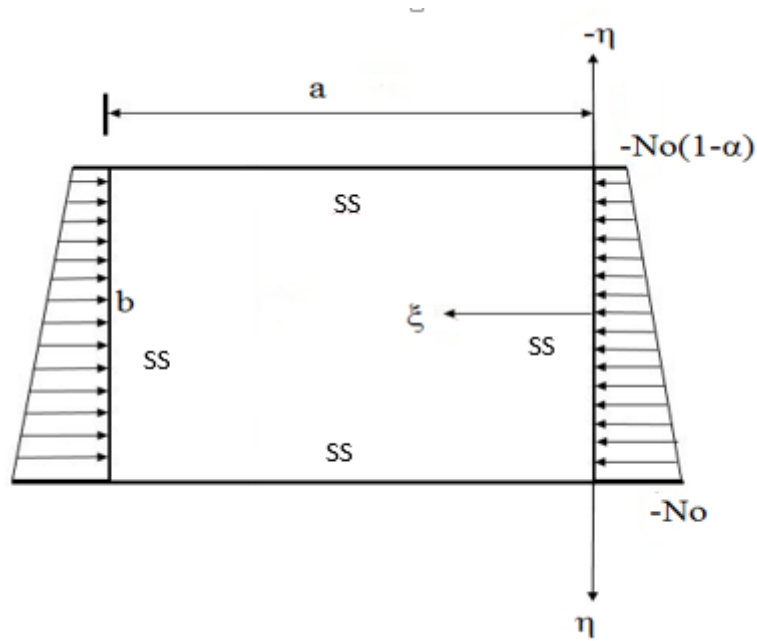
(i.b)

**Fig A.i. Non dimensional representation of geometry of the plate with uniformly varying load along ξ direction**

The first of these equations, sometimes called the "Compatibility Equation" ensures that in an elastic plate the in-plane and out-of-plane displacements are compatible. The second equation is based on equilibrium principles, and is sometimes termed the "Equilibrium Equation". Exact solution of these equations is only possible for the simplest loading and support conditions, but solutions which are within reasonable accuracy are obtainable for a wide range of problems.

Here x, y, z are the set of Cartesian co-ordinates with xy in the middle surface of the plate in un deformed condition, w is the normal deflection parallel to z direction in the middle surface of the plate, t is the uniform thickness of the plate, D is the flexural stiffness and F an Airy's stress function which gives direct stresses $\sigma_x$, $\sigma_y$

$$D = Et^3/12(1-\gamma^2) \tag{ii}$$

$$\sigma_x = \partial^2 F/\partial y^2 \tag{iii}$$

$$\sigma_y = \partial^2 F / \partial x^2 \tag{iv}$$

$$\tau_{xy} = -\partial^2 F / \partial x \partial y \tag{v}$$

For applying Galerkin method in von Karman equation the terms in equations need to be converted to non-dimensional form. Writing equation (4.2) in non-dimensional form by substituting

$\xi = x/l$, $\eta = y/b$, $\varphi = l/b$, $\omega = w/t$, $F' = F/Et^2$

Where l is the plate length in x direction and b the plate breadth in y direction. Equation (4.1) then becomes

$$1/\varphi^2\, \partial^4\omega/\partial\xi^4 + 2\, \partial^4\omega/\partial\xi^2\partial\eta^2 + \varphi^2\, \partial^4\omega/\partial\eta^4 = 12(1-\gamma^2)\, [\partial^2 F/\partial\eta^2\, \partial^2\omega/\partial\xi^2 + \partial^2 F/\partial x^2\, \partial^2\omega/\partial\eta^2 - 2\partial^2 F/\partial\xi\partial\eta\, \partial^2\omega/\partial\xi\partial\eta] \tag{vi}$$

$$1/\varphi^2\, \partial^4 F/\partial\xi^4 + 2\partial^4 F/\partial\xi^2\partial\eta^2 + \varphi^2\partial^4 F/\partial\eta^4 = [(\partial^2\omega/\partial\xi\partial\eta)^2 - \partial^2\omega/\partial\eta^2\, \partial^2\omega/\partial\xi^2] \tag{vii}$$

An exact solution of the above problem is impossible. Hence an approximate solution for this equation is to be found using Galerkin's method.

## A.2 Galerkin series derivation for stress function

A rectangular plate which is initially flat with the four edges simply supported is considered. The plate is loaded by a uniformly varying load along two simply supported edges. The formulation is fully done in non-dimensional form. At $\xi = 0$ and $\xi = 1$ the imposed boundary conditions for stress functions are

$$\sigma_{x\,(,x=0,l)} = No/t[(1-\alpha/2) + \alpha y/b] \tag{viii}$$

The above equation in non-dimensional form gives

$$\sigma_{\xi\,(,\xi=0,1)} = \partial^2 F'/\partial\eta^2{}_{(\xi=0,1)} = No'[(1-\alpha/2) + \alpha\eta] \tag{ix}$$

$\tau_{\xi\eta(,\xi=0,1)}=0$

Where $N_o'=N_o l^2/\varphi^2 E t^3$

The normal and shear stresses along the unloaded edges are zero.

$\tau_{\eta\xi(\eta=-1/2,+1/2)} = \partial^2 F'/\partial\xi\,\partial\eta\,_{(\eta=-1/2,+1/2)}=0$         (xi)

$\sigma_{\eta\,(\eta=-1/2,+1/2)} = \partial^2 F'/\partial\xi^2{}_{(\eta=-1/2,+1/2)}=0$         (xii)

An approximation for the stress function is such that at the loaded edges the stress function returns the assumed value of direct stresses.

Then the assumed form of the stress function can be written as

$F'=No'/2[(1-\alpha/2) + \alpha/3\eta]\,\eta2+ \sum_r\sum_s b_{rs}\,f_r(\xi)\,g_s(\eta)$     (xiii)

Hence assume $f_r(\xi)$ as

$f_r(\xi)=\sin^2 r\Pi\xi$         (xiv)

A polynomial function is chosen for $g_s(\eta)$

$g_s(\eta)= g_s(\eta)= \eta^{s+4} +As\,\eta^{s+3}+Bs\,\eta^{s+2}+Cs\,\eta^{s+2}+Ds\,\eta^s$     (xv)

Substituting for $\sigma_\xi$ in equation (xi) and (xii) applying boundary conditions, possible forms of solutions of $g_s(\eta)$ are,

$g_s(\eta)= \eta^{s+4} -.5\,\eta^{s+2}+ 1/16Ds\,\eta^s$         (xvi)

Substituting the obtained values of $f_r(\xi)$ and $g_s(\eta)$ in equation (6) gives the value of F' as

$F'= No'/2[(1-\alpha/2) + \alpha/3\eta]\,\eta2 + \sum_{r=1,2}^{T}\sum_{s=0,1}^{U} brs\,\sin r\Pi\,\xi2\,[\eta^{s+4} -.5\,\eta^{s+2} + $

$1/16Ds\,\eta^s]$         (xvii)

## A.3 Galerkin series derivation for deflection function

The four edges of the plate are assumed to be simply supported. Hence moment is zero at other edges. Hence for loaded edges the boundary conditions expressed in non-dimensional form is

$$M_{\xi(\xi=0,1)}=[\partial^2\omega/\partial\xi^2+\gamma\ \varphi^2\partial^2\omega/\partial\eta^2]_{(\xi=0,1)}\ =0 \qquad\qquad \text{(xviii)}$$

$$\omega_{\ \xi(\xi=0,1)}=0 \qquad\qquad \text{(xix)}$$

For unloaded edges

$$[\partial^2\omega/\partial\eta^2+\gamma\ /\varphi^2\ \partial^2\omega/\partial\xi^2]_{(\eta=-1/2)}\ =0 \qquad\qquad \text{(xx)}$$

$$[\partial^2\omega/\partial\eta^2+\gamma\ /\varphi^2\ \partial^2\omega/\partial\xi^2]_{(\eta=+1/2)}\ =0 \qquad\qquad \text{(xxi)}$$

Now an approximation for $\omega$ satisfying the boundary conditions given by equations xviii to xxi are to be found out. Assuming $f_m(\xi)$ and $g_m(\eta)$ as two independent functions of $\xi$ and $\eta$ respectively the deflection function is assumed as

$$\omega=q_{mn}\ f_m(\xi)g_m(\eta) \qquad\qquad \text{(xxii)}$$

Where $q_{mn}$ are constants. Assumed forms of $f_m(\xi)$ and $g_m(\eta)$ are

$$f_m(\xi)=\sin m\pi\ \xi \qquad\qquad \text{(xxiii)}$$

$$g_m(\eta)=\eta^{n+4}+A_n\eta^{n+3}+B_n\eta^{n+2}+C_n\eta^{n+1}+D_n\eta^n \qquad\qquad \text{(xxiv)}$$

Solving the above equations the coefficients $A_n$, $B_n$, $C_n$ and $D_n$ are found out. Back substituting the obtained values of coefficients in the series form of deflection function gives the expression for deflection function ($\omega$). This series approximation of deflection function is substituted in von Karman governing differential equations along with the series form of stress function and solved for unknown coefficients.

## A.4 FORMULATION OF POSTBUCKLING SOLUTION

As the solution strategy given by A.C walker was found to be erroneous an independent solution methodology was developed. The Galerkin series stress and deflection function were derived Walker 1967 as

F'= No'/2[(1-α/2) + α/3η] η2 + $\sum_{r=1,2}^{T} \sum_{s=0,1}^{U}$ brs sin rπ ξ [$\eta^{s+4}$ − .5 $\eta^{s+2}$ +

  1/16Ds $\eta^{s}$]                                          (xxv)

ω =$\sum_{m=1,2}^{p} \sum_{n=0,1}^{L}$ sin mπ ξ $q_{mn}$ [$\eta^{n+4}$ + $A_{n}\eta^{n+3}$ + $B_{n}\eta^{n+2}$ + $C_{n}\eta^{n+1}$ + $D_{n}\eta^{n}$]

In the deflection equation m corresponds to the buckling mode. Fixing a value for m simplifies the double summation series to a series of single summation. Hence

ω = $\sum_{n=0,1}^{L}$ sin mπ ξ $q_{n}$[$\eta^{n+4}$ + $A_{n}\eta^{n+3}$ + $B_{n}\eta^{n+2}$ + $C_{n}\eta^{n+1}$ + $D_{n}\eta^{n}$ ]       (xxvi)

Generalized term of the stress and deflection function is represented as

$F_{pq}$=$b_{pq}$sin²rπξ [$\eta^{s+4}$ − .5 $\eta^{s+2}$ + 1/16Ds $\eta^{s}$]            (xxvii)

$\omega_{i}$ = $q_{i}$ [$\eta^{i+4}$ + $A_{i}\eta^{i+3}$ + $B_{i}\eta^{i+2}$ + $C_{i}\eta^{i+1}$ + $D_{i}\eta^{i}$]           (xxviii)

Applying Galerkin method to the von Karman equation gives

$\sum_{n=0,1}^{L} \sum_{r=1,2}^{T} \sum_{s=0}^{U} \int_{0}^{1} \int_{-.5}^{.5}$[1/φ² ∂⁴F/ ∂ξ⁴ + 2 ∂⁴F/ ∂ξ² ∂η²+ φ² ∂⁴F/ ∂ η⁴ −

  (∂²ω/ ∂ξ ∂η)² + ∂²ω/ ∂η² ∂²ω/ ∂ξ²]d$F_{pq}$/db$_{pq}$dξdη=0          (xxix)

$\sum_{n=0,1}^{L} \sum_{r=1,2}^{T} \sum_{s=0}^{U} \int_{0}^{1} \int_{-.5}^{.5}$[1/φ² ∂⁴ω/ ∂ξ⁴ + 2 ∂⁴ω/ ∂ξ² ∂η²+ φ² ∂⁴ω/

∂ η⁴ −12(1-γ²) [∂²F/∂η² ∂²ω/∂ξ² +∂²F/∂x² ∂²ω/∂η² -2∂²F/∂ξ∂η ∂²ω/∂ξ∂η] dωi/dqi

dξdη=0                                                   (xxx)

The above simultaneous equation is solved in Matlab software. Iterating the values of n, r and s generates a set of nonlinear simultaneous equations. Equations (5.5) and (5.6) are expressed in matrix form to simplify the problem.

$[A]\ b_{rs} = [B]\ [q_i\ q_i]$ (xxxi)

$[C]\ [q_i] = [D]\ [b_{rs}\ q_k]$ (xxxii)

Equation expressed in matrix form gives

$[A]_{TU*TU}\ b_{rs} = [B]_{TU*LL}\ [q_i^2]$   Hence

$b_{rs} = [A]_{TU*TU}{}^{-1}[B]_{TU*LL}\ [q_i q_i]$ (xxxiii)

Equation 22 expressed in matrix form gives

$[C]_{L*L}\ [q_i] = [D]_{L*TUL}\ [b_{rs}q_k]$ (xxxiv)

Substituting for $b_{rs}$ in equation 34 gives

$[C]_{L*L}\ [q_i] = [D]_{L*TUL}\ *([A]_{TU*TU}{}^{-1}\ [B]_{TU*LL})\ *[q_i^2]\ [q_k]$ (xxxv)

Hence,

$[q_i] = ([C]_{L*L}{}^{-1}\ [D]_{L*TUL}\ )*([A]_{TU*TU}{}^{-1}\ [B]_{TU*LL})\ [q_i^2]\ [q_k]$ (xxxvi)

The simultaneous equation which earlier contained $b_{rs}$ and $q_n$ as the unknown coefficients is now reduced to a set of nonlinear equations with a single unknown coefficient $q_n$. The above nonlinear equation is solved using the solver in Matlab.

## A.5.RESULTS AND DISCUSSION

As evident from fig 6.1 and 6.2 the plots are in agreement with the results from A.C. Walker paper. The applied compressive load against stress plot is linear till it reaches the elastic buckling load and then increases non-linearly. This is due to the

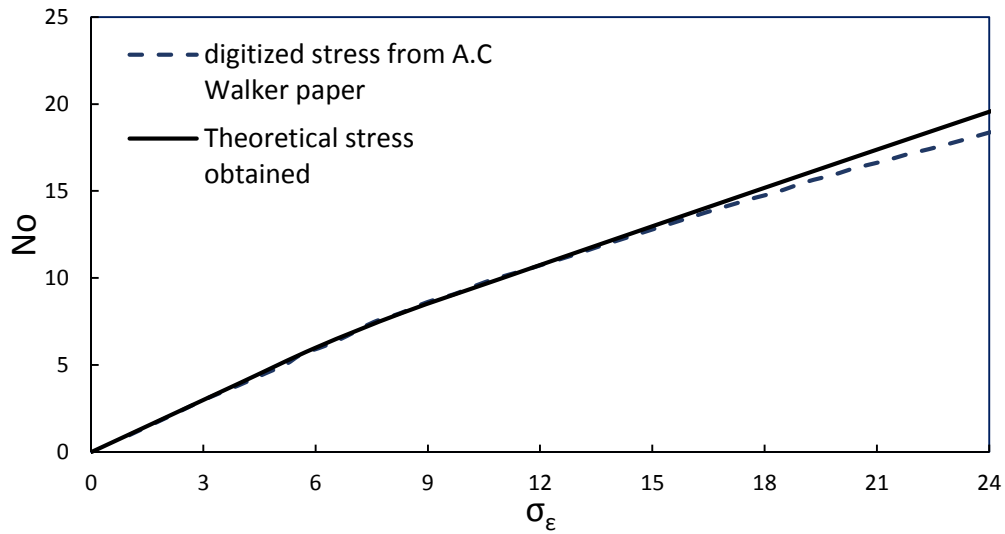effect of terms from deflection series which becomes prominent after elastic buckling load.



**Fig.A.ii Comparison of obtained value of edge stress with Walker (1967) for**
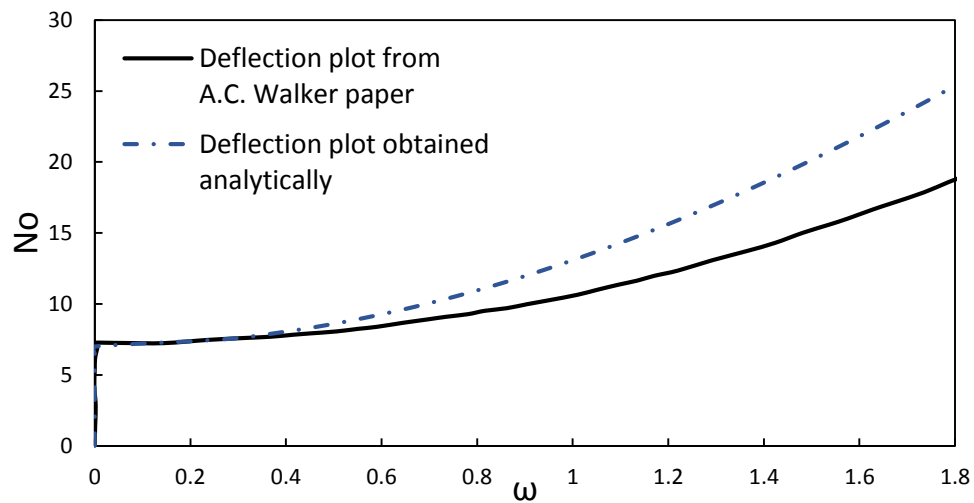
**m=2, α=1 and φ=2**



**Fig.A.iii Comparison of obtained value of deflection with A.C. Walker paper**
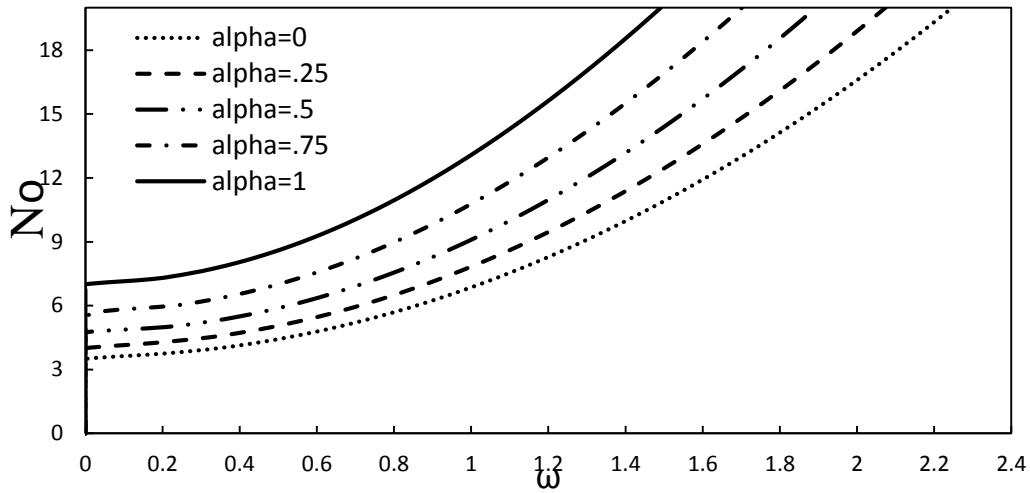
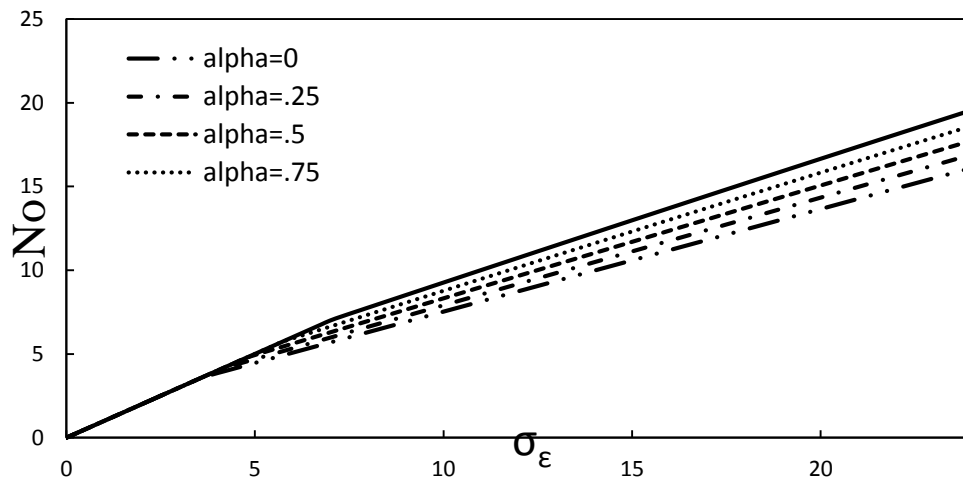**Fig. A. iv Load-Deflection plot for varying values of load eccentricity parameter**



**Fig. A.v Stress plot for varying values of load eccentricity parameter**

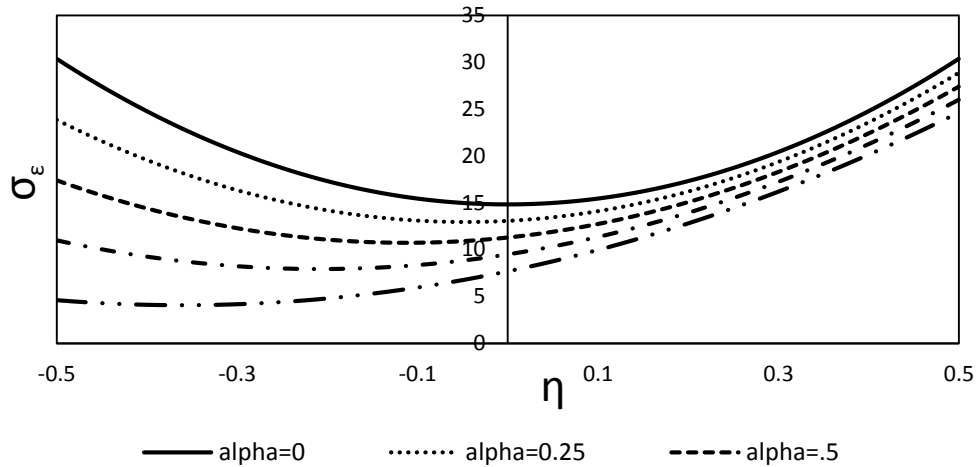Legend: —— alpha=0    ⋯⋯⋯ alpha=0.25    ‑‑‑‑‑ alpha=.5

**Fig.A.vi Variation of transverse stress for varying values of load eccentricity parameter**

The term alpha in figure 6.3 to 6.5 corresponds to the load eccentricity parameter. The edge stress can be considered to be in inverse relation. This is because with the increase of value of $\alpha$, the total compressive load acting on the edge decreases. This effect will be more towards the edge where the stress intensity is minimum.



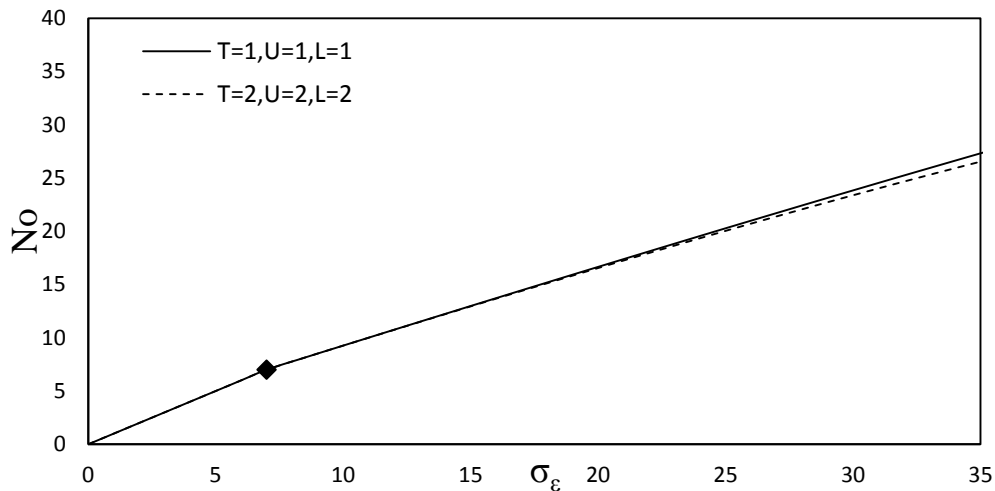**Fig.A.vii Effect of varying number of terms in edge compressive stress**
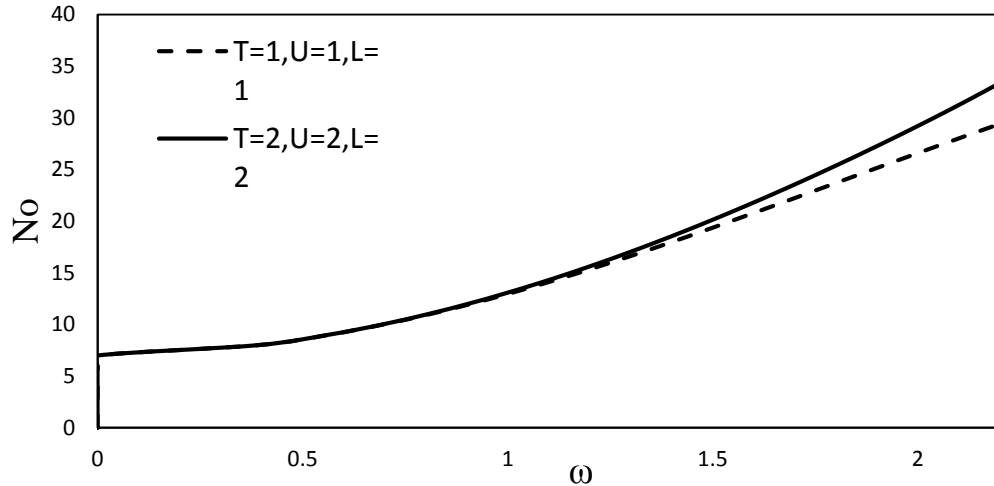
**Fig.A.viii Effect of increased number of terms in deflection variation**

In the initial phase the calculations were done with number of terms included in the deflection as well as stress function series. But with the inclusion of more number of terms the deflection as well a stress profiles seem to be getting more and more accurate. This phenomenon is observed when the applied load is greater than the Elastic buckling load. This is because when the applied load is less than elastic buckling load the series part of stress function is absent.
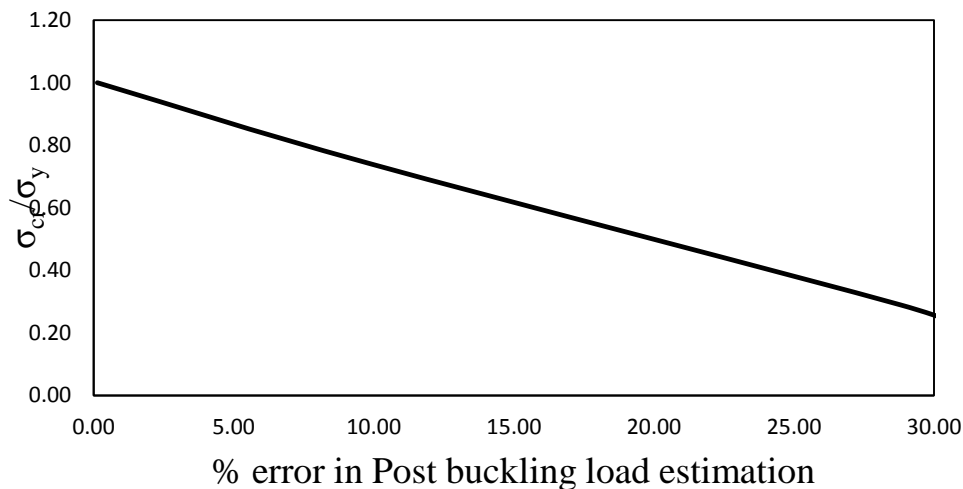


**Fig. A.xi Comparison of obtained Post buckling load with load based on von Karman equation**

Fig 6.8 represents the relation between $\sigma_{cr}$ and effective width estimation by von Karman. The von Karman effective width expression is given as

$$b_e/b=\sqrt{\sigma_{cr}/\sigma_y} \quad . \tag{xxxvii}$$

A modified expression for von Karman's effective width expression was suggested by Winter. When the stress at the outer strips reaches the yield stress, the corresponding effective width can be calculated using Winter's formula

$$b_e/b=\sqrt{(\sigma_{cr}/\sigma_y)} \; (1\text{-}0.25\sqrt{(\sigma_{cr}/\sigma_y)}) \tag{xxxviii}$$

Based on effective width the post buckling strength of the plate is calculated. When the value of $\sigma_{cr}$ approaches $\sigma_y$ the error in the effective width calculation reaches minimum.

The verification of obtained results was initiated by imposing condition of uniform compression. The elastic buckling load is obtained from the load deflection plot. With the increase in applied load the deflection was initially zero. But when the applied compressive load reaches a particular point the deflection was found to increase drastically, which is the elastic buckling load. The obtained results were compared with the available theoretical prediction and was found to be in excellent agreement with the values.